Dynamical Climatology

A model simulation of the seasonal cycle in the tropical Pacific Ocean using climatological and modelled surface forcing.

by

C. Gordon and R.A. Corry

DCTN 78

July 1989

Meteorological Office (Met. O. 20)
London Road
Bracknell
Berkshire RG12 2SZ

DYNAMICAL CLIMATOLOGY TECHNICAL NOTE NO. 78

A MODEL SIMULATION OF THE SEASONAL CYCLE IN THE TROPICAL PACIFIC OCEAN USING CLIMATOLOGICAL AND MODELLED SURFACE FORCING

by

C Gordon and R A Corry

Met O 20 (Dynamical
Climatology Branch)
Meteorological Office
London Road
Bracknell
Berkshire, UK RG12 2SZ

July 1989

NOTE: This paper has not been published. Permission to quote from it should be obtained from the Assistant Director of the above Meteorological Office branch.

1. INTRODUCTION

It has been recognised for some time that the El Nino - Southern Oscillation (ENSO) phenomena involves coupled ocean - atmosphere dynamics and thermodynamics (Bjerknes, 1966). In recent years the development of large General Circulation Models (GCMs) of the atmosphere and ocean has meant that a detailed simulation of this complex system with sophisticated models may now be possible. Evidence from atmospheric models suggests that the currently available atmospheric GCMs are capable of responding realistically, at least within the tropical belt, to prescribed Sea Surface Temperature (SST) anomalies in the tropical Pacific (Shukla and Blackmon, 1986). The reverse problem of modelling the response of the near surface ocean structure to prescribed wind forcing anomalies has also been studied with a number of tropical Pacific ocean GCMs and these experiments also indicate that the ocean models have considerable skill in simulating the observed ocean conditions (Philander and Seigel, 1985; Latif, 1987). Taken together, the recent results from atmospheric and oceanic modelling suggest that a coupled GCM of the tropical Pacific ocean and global atmosphere should be capable of simulating the interactions taking place during an ENSO episode. A model of this kind is described in Gordon, 1988.

The atmosphere and ocean exchange heat and momentum across the air - sea interface and these fluxes provide one of the primary forcing mechanisms of both the ocean and atmosphere systems. The oceanic and atmospheric models are, however, likely to have systematic errors which can lead to significant deficiencies in surface flux simulations by the atmospheric models when forced with prescribed SSTs and in SST simulations by the ocean models when forced with prescribed surface fluxes. Even if the atmospheric model is provided with perfect SSTs it will not produce perfect flux simulations due to inevitable limitations in the model formulation. Similarly, ocean models supplied with perfect surface forcing will not produce perfect SSTs although it is likely that as both the atmospheric and oceanic models models are developed further these systematic errors will be reduced.

It is useful to estimate the magnitude and significance of these surface flux errors. The former could be done by comparing with observed quantities - if these were available. The spread in climatological estimates is rather large and, in fact, for the atmospheric model discussed in this paper, the climatology of surface fluxes produced by the model is within the uncertainty of current observed estimates over most of the tropical Pacific. To assess the significance of the surface flux errors requires an ocean model since the significance is here measured by the errors arising from the ocean model as a consequence of these surface forcing errors.

The sensitivity of the models to systematic errors in the forcing can be studied in a fairly straightforward manner. Numerous SST anomaly experiments have been performed with atmospheric GCMs. Fewer experiments have been carried out with ocean models and the only extensive study is that of Harrison (1988) in which different wind analyses for the 1982/83 El Nino event were used to drive the tropical Pacific model of Philander and Seigel (1985). In the absence of sufficiently accurate climatologies the best way to assess GCM flux products is to use them to drive an ocean model and to compare the resultant oceanic fields with those produced from a simulation with climatological fluxes and with ocean data.

This paper addresses the following questions: How well can an ocean GCM simulate the seasonal cycle in the tropical Pacific when forced with climatological estimates of the surface forcing? How does the simulation change when the observed climatology is replaced by a climatology defined by an atmospheric model? In particular we will be interested in the simulation of near surface conditions and SST. Answering the first question provides insight into how the ocean model responds and the typical errors that are encountered. The second question addresses the issue of sensitivity of the ocean response. The fluxes from the atmospheric model are known to be within the error envelope of the observed estimates and these experiments give an indication of the significance of these errors in terms of their effect on the ocean model simulation. Despite the limiting assumptions that are made regarding the atmospheric feedback, non-interactive experiments of the kind described below are of considerable

value when interpreting the response of the fully coupled model. It is most unlikely that systematic errors in atmospheric models will be removed by introducing an interactive ocean as evidenced by comparing the non-interactive results presented here with the ENSO simulation in Gordon, 1988. The simulation with prescribed fluxes gives a reasonable first order estimate of the initial response of the ocean model in the coupled system.

From a single experiment it is difficult to assess whether inadequacies in the simulation are due to the model physics or due to the uncertainty in the surface forcing. By comparing these two experiments using the same model but different forcing further insight is obtained that can help to disentangle the errors arising from these two sources.

This paper is organised as follows: Section 2 describes the ocean model and Section 3 the surface forcing from both climatology and the atmospheric GCM together with the observed seasonal cycle in SST. Results from the ocean model when forced with precribed climatological fluxes and those from the AGCM are described in Sections 4 and 5 respectively. In Section 6 the results obtained are briefly compared with those from other model studies of the seasonal cycle. Finally, results are summarized and conclusions drawn in Section 7.

2. THE OCEAN MODEL

The ocean model is a high resolution version of the Bryan/Cox model (Cox, 1984) covering the tropical Pacific ocean between 30°N and 30°S. The latitudinal resolution is 1 degree at the northern and southern boundaries, reducing smoothly to about 1/3 degree on the equator. The longitudinal resolution is 1½ degrees in the central Pacific, reducing to 1/2 degree at the coasts (the western boundary is closed in the model). The horizontal eddy viscosity varies with the grid spacing so that in the finer regions of the grid a smaller diffusion coefficient is used (the minimum value is 2×10^7) which avoids excessive diffusion in the finer regions of the grid near the equator and coasts. The lateral eddy diffusivity for temperature

and salinity is held constant at a value of 2×10^7 $cm^2 s^{-1}$ throughout the grid. Salinity effects are included in the model but the barotropic part is not included. The main emphasis of these experiments focuses on variations in the upper ocean, particularly on the thermal structure, and since tests showed the barotropic current to be typically an order of magnitude less than the near-surface baroclinic current it will not contribute significantly to the near surface advection of heat and the evolution of SST. The ocean model coastline is a little different from the true coastline at the model resolution. This is because the ocean model used in this this study is the same as that used in coupled GCM studies and the coastline geometry was chosen to match that of the atmopheric model. In order to reduce the computer storage required by the ocean model the eastern coastline is distorted south of the equator so that the model coastline lies directly north - south rather than following the South American coast. There are 16 levels in the vertical with a 10m resolution near the surface and there is a constant ocean depth of 4000m. The K-theory mixing scheme of Pacanowski and Philander (1981) is used to parametrize vertical turbulent mixing but with lower values of the stability independent background mixing as suggested by Gregg et al (1985). To avoid a numerical instability arising from the vertical diffusion calculation an iterative procedure is used in the diffusive calculation, so effectively reducing the timestep in this part of the model.

Open boundary conditions in temperature, salinity and momentum are applied at 30°N and 30°S and the effect of these is to keep the longitude - depth profiles of temperature and salinity on the boundary close to their seasonally varying climatological values as specified by Levitus (1982). This is achieved by making the meridional temperature (salinity) gradient at the boundary proportional to the difference between the predicted and climatological temperature (salinity) at all depths. The constant of proportionality is chosen to ensure the boundary values remain close to their climatological values. The meridional gradient of both current components is set equal to zero at the boundary. In the upper levels this allows (in general) an Ekman drift across the boundaries at 30°N and 30°S. Since the barotropic part is set to zero in the model there is no net mass flux across the boundaries although there can be a net heat flux. These

boundary conditions also damp coastal Kelvin waves travelling polewards along the eastern boundary (Gordon, 1986) and allow a net heat flux across the boundary.

The net surface heat flux (Q) is parametrized by

$$Q(T)=Q(T_c)+\lambda(T_c-T) \qquad (1)$$

$$\lambda=-\partial Q/\partial T$$

where $Q(T_c)$ is the heat flux at the climatological SST (T_c) and T is the surface (actually 5m) temperature predicted by the ocean model. The penetrative part of the short wave flux is treated separately as explained below. The second term in (1) allows for the local negative feedback towards climatology due to the temperature dependence of the heat loss from the ocean surface. The formulation given in (1) is identical to that of Haney (1971) and Haney's effective air temperature (T_{air}^{eff}) is obtained by equating (1) with $\lambda(T_{air}^{eff}-T)$. The feedback parameter λ is assigned a value of 35 Wm-2K-1 which is appropriate to the tropical regions. For a 50m mixed layer depth this value corresponds to a relaxation time of approximately 2 months. The SST simulation is sensitive to the value of λ and in the limit of infinite λ the climatological temperatures are regained. Experiments have been performed with a number of values for λ, both higher and lower, and although the SSTs are different in each case the spatial patterns are essentially the same. (A particularly interesting experimemt was one in which the model SST was replaced each timestep with the seasonally varying climatological value, a procedure which is equivalent to setting $\lambda=\infty$. The implied net surface heat flux was then derived as a diagnostic quantity. However, although by specification the SST field was perfect, a very unrealistic vertical thermal structure was produced in areas of strong upwelling.)

The Haney formulation used in (1) is inadequate in many respects. Both studies with externally specified forcing data (Wells and Kin-Hele, 1988: Gautier, private communication) and coupled GCM experiments (Gordon, 1988) have indicated that the effects of wind variations on the latent heat loss

and cloud variations on the short wave flux are both first order effects when considering changes in net surface heating. The value of 35Wm-2K-1 for the Haney coefficient arises from an assumption of constant air temperature and wind speed in the tropics - independent of SST.

A number of authors (e.g. Schopf, 1983, Philander and Seigel, 1985) have pointed out that the assumption of a fixed air temperature is generally unrealistic and that in practice the air temperature follows the SST very closely. A better parametrization is often thought to arise by assuming a constant air - sea temperature difference so that the implied Haney coefficient (i.e. $-\partial Q/\partial T$) is considerably smaller and in the range 5 - 15 Wm-2K-1. These values of λ also imply considerably longer decay timescales for SST anomalies and these are more consistent with observed decay times. (However, it is not clear that in reality the only significant mechanism in the decay of large scale SST anomalies is local heat exchange.) These heat flux schemes with a constant air-sea temperature difference tend to produce excessively high SSTs in regions of low winds and this is usually compensated for by assuming a rather high minimum wind speed to represent short time-scale wind variability. As noted previously, cloud shading effects are probably important. In the coupled model of Gordon (1988) there are large changes in cloud in regions of low level convergence - which also tend to be regions of low winds. When the cloud effect is taken into account the Haney coefficient is again increased (at least in convective regions), often to a values above 35Wm-2K-1. The form of the feedback term in (1) was chosen because it is simple and its effects on the simulation are easily assessed. A proper treatment of the heat flux should include the dependence of Q on temperature, wind and cloud variations and this complexity is best dealt with in the context of coupled models. In the experiments reported here the same value of λ is used with both climatological and atmospheric GCM values of $Q(T_c)$.

When written in the form (1), it is clear that the parametrization is such that the heat flux into the ocean has its climatological value when the modelled temperature is equal to the climatological temperature. Spatial and seasonal variations are included in $Q(T_c)$. In the case of AGCM fluxes

this correspond to the fluxes produced by the model when climatological SSTs are used at the ocean surface throughout the integration.

In the ocean model the shortwave radiative component of the surface heating is allowed to penetrate below the top model layer and a constant Jerlov optical water type IB is used throughout the domain. Below the surface the shortwave flux is attenuated using a 'two band' approximation given by $S/S_o=R\exp(\eta_1 z)+(1-R)\exp(\eta_2 z)$ where S is the flux at a depth z, S_o the surface flux and R, η_1 and η_2 are deterined from data from a specific water type (Paulson and Simpson, 1977).

The fresh water flux at the surface is also formulated in the form (1) but with temperature replaced by salinity and the feedback parameter chosen to give the same time scale of adjustment as the temperature relaxation time associated with λ. Although there is no physical basis for this fresh water feedback it is used to ensure that the surface salinities remain close to their climatological values as specified from Levitus (1982). The adjustment time was chosen to be the same for temperature and salinity since different times can lead to unrealistic T-S relationships (MacVean, private communication). In this study, the fresh water flux from the AGCM simulation is not used since our primary concern is with thermal effects although the dynamical effects of salinity may not be negligible (Cooper, 1987).

The ocean model was initialised using the Levitus (1982) temperature and salinity fields for September and zero currents. The seasonally varying surface forcing and zonal boundary profiles at 30°N and 30°S of temperature and salinity were updated every 3 days throughout the integration. The 3-day values were obtained by linear interpolation in time from the monthly mean surface flux and Levitus datasets. The model was integrated for 4 years using the climatological fluxes and by the end of this time the upper ocean had essentially reached equilibrium. The model was then integrated for a further year using the fluxes derived from the atmospheric GCM.

3. THE FORCING FLUXES AND THE OBSERVED SEASONAL CYCLE IN SST

Experiments have been performed with two sets of forcing fluxes. In the first, the wind stress analysis of Hellerman and Rosenstein (1983) and the surface heat flux climatology of Esbensen and Kushnir (1981) were used. The second set of forcing fields were derived from a four year integration of the United Kingdom Meteorological Office (UKMO) atmospheric GCM (Slingo et al, 1988). A mean dataset for each month was compiled from the four individual years and this monthly forcing was used to drive the ocean model. The annual mean model fluxes were compared with various climatological estimates by Gordon (1989) and have been generally found to be within the uncertainty in these estimates. Figs. 1 and 2 show the climatological SST (UKMO analysis), Hellerman and Rosenstein (HR) wind stresses and the Esbensen and Kushnir (EK) net surface heat flux for March and September respectively. The fresh water flux was calculated from the EK latent heat fluxes with Jaeger's (1976) precipitation climatology (not shown).

In response to the seasonal variations in surface forcing there are substantial changes in near surface ocean temperatures and currents. It can be seen from figs. 1a and 2a that the warm pool in the west Pacific migrates with the sun, so that in March the warmest water is south of the equator whereas in September it is in the northern hemisphere. The cold water on the equator due to upwelling is evident as far west as the date line in both months but is more pronounced in September. The plots shown in figs. 1a and 2a are produced from fields on a 2.5°×3.75° latitude-longitude grid (the atmospheric GCM grid). The analysis of SSTs on a finer 1°×1° grid performed by Reynolds (1982) shows colder upwelled water on the equator and evidence for upwelling in the SSTs further west. The smoothing implied in figs. 1a and 2a because of the 2.5° latitudinal spacing removes some of this detail.

The cold tongue in the east Pacific has its maximum extent in September/October and minimum in March/April. This is due to the seasonal variation in the strength of the SE trades shown in figs. 1b and 2b, which cause large seasonal variations, primarily in equatorial upwelling but also

in lateral heat advection by the South Equatorial Current (SEC) and in surface heating (Enfield, 1986). The net surface heat fluxes are shown in figs. 3a and 3b from the EK climatology. In the east Pacific the heat fluxes vary from 120 Wm-2 in March to 80 Wm-2 in September and this difference is mainly associated with the different low level winds at these times. SSTs are higher and net heat input into the ocean is larger in March than September. The winds are higher in September than March and the reduction in evaporation in March due to the wind effect is more important than the effect of the relatively warmer SSTs. Cloud feedback is also significant and probably accounts for the shifted position of the heating maximum between March and September. Low cloud forms over the coldest water in the far east in September and so reduces the shortwave flux. The cloud amounts are lower and less extensive in March so that the maximum heating region is nearer the coast (Weare et al, 1980).

In the west Pacific there is a relatively small seasonal cycle in surface heating and away from the equator the heat fluxes essentially follow the sun. In these areas most of the seasonal variation in SST can be explained in terms of changes in heat input and mixed layer depth (or surface mixing). Grahame (1984) calculated the global distribution of the implied seasonal range of SST using EK fluxes and observed seasonal sycle in mixed layer depths and in the areas noted above this agreed well with the observed range.

Currents derived from ship drift data show the North Equatorial Counter Current (NECC) at most longitudes to be strongest around September and weakest around March. The SSTs under the ITCZ are typically 1°C warmer in September than in March although according to the data of Taylor (1973) and Shea (1986) this does not lead to increased precipitation in the central Pacific ITCZ in September relative to March. This is presumably because the moisture in the ITCZ arises from convergence of the moist air in the trade wind systems rather than primarily from local evaporation. (In the east Pacific the precipitation is more intense in September.) It is interesting that the warmer SSTs in September under the convergence zone are, in part (local wind effects on evaporation are also important), due to the increased strength of the NECC which is forced by the large wind curl

to the north of the ITCZ and the oceanic mass convergence between the equator and 10°N. In the region between the equator and the ITCZ the mass convergence is caused by the reduction in poleward Ekman transport due to both decreasing winds and an increasing Coriolis effect. The low easterly wind stress in the ITCZ is also relevant since the NECC has a subsurface maximum and decreases towards the surface due to the input of easterly momentum by the wind. When the winds are light the maximum can move towards the surface and enhance the heat advection from the west. In a rather complicated way the positioning and strength of the ITCZ and the NECC are intrinsically linked, each providing partial forcing for the other. It will be possible to investigate this connection further by the use of coupled models.

The wind stress and surface heat flux derived from a four year integration of the UKMO atmospheric GCM are shown in figs. 3 and 4. It should be emphasised that the HR and EK climatologies should not be regarded as definitive but rather as representative of observed estimates. The major differences between the model fluxes and HR and EK will be noted here but the reader is referred to Gordon (1988) for a more complete discussion as to the possible cause of these differences.

In both March and September the model stresses in figs. 3a and 4a are generally lower than HR. The model fields also have stronger gradients to the north of the ITCZ in each month and particularly low stress magnitudes under the ITCZ in September. In September the region of the maximum stress in the NE trades is south of its position in HR. Along the equator in the eastern and central Pacific the model stresses are typically 20 - 30% lower in the model than in HR. One major difference between the calculation of the stresses in the model and by HR is the lower drag coefficient used in the model. The model uses a coefficient equivalent in neutral conditions to a 10m value of 1.2×10^{-3} whereas HR use values around 1.5×10^{-3} in the tropical Pacific (the HR drag coefficient is also wind and stability dependent).

The model net surface heat flux for March, shown in fig. 3b, exhibits the same overall pattern as the EK flux in fig. 1c. The model has peak values

of 140 Wm-2 centred around 120°W in the east Pacific and average values of around 60 Wm-2 in the west Pacific (compared to values of around 30Wm-2 in EK). In September the maximum in the east is against the coast rather than around 120°W as in EK. This may be due to an underestimation of the low cloud in the model in the east Pacific. The model does produce cloud against the coast (Slingo et al, 1988) but the amounts are low, typically 60% cover whereas Weare et al (1980) suggest a total cloud cover of 70 - 80% in this area. In the NE tropical Pacific the model has a net heat input into the ocean whereas EK show this as a region of net surface cooling, however, the model does show a net cooling under the trade wind maxima in both hemispheres. In the west, between 5 - 10°N, the model field for September has a region of large heat input with fluxes of 80 - 100 Wm-2 into the ocean (fig. 4b). Further analysis of the atmospheric GCM response shows light low level winds (less than 2.5ms-1 at 850mb) in this area and correspondingly low evaporation rates.

The above has been a descriptive account of the net model fluxes and their comparison with those from the HR and EK climatologies. More accurate climatologies are required before a detailed assessment of the different heat flux components (latent, short wave etc) from the model will be possible.

4. RESULTS WITH CLIMATOLOGICAL FORCING

In this section monthly mean results from the fourth year of the model integration with HR stresses and EK fluxes will be described. After four years of integration the model has obtained equilibrium in the sense that the near surface monthly mean fields for the fourth year are essentially the same as those for the third year. The day to day fields are not the same due to instabilities in the flow, and these are most energetic in the high gradient region in the eastern Pacific just north of the equator.

The modelled SST for March is shown in fig. 5a and should be compared to the climatology for this month in fig. 1a. The fields compare well except in the equatorial east Pacific near 120°W where the model values are 2 - 3°C

too cold. In comparing the SST fields it should be remembered that the model SST is forced back towards the climatological value by the surface Haney forcing. Fig.5b shows the contribution to the total March monthly mean heat flux arising from the Haney feedback term (second term in (1)). If the contribution of this term is small compared with the EK heat flux in fig.1c (first term in (1)) then the conclusion can be drawn that the EK fluxes, with the HR wind stresses, are the fluxes required by the ocean model to reproduce the climatological SST. Outside of the central and eastern equatorial region the contribution from the feedback term is generally in the range 0 - ±20 Wm-2 whereas the EK values are 0 - ±40 Wm-2. The largest feedback contribution occurs in the eastern central Pacific where the value is larger than 80 Wm-2 over the cold water on the equator. The possible causes of the large SST errors in this region are:

(a) The ocean model cannot properly handle the physics required for the heat budget in this area.

(b) The heat flux into the ocean is too low.

(c) The zonal easterly wind stress on the equator is too high leading to too much upwelling of cold water.

Both (b) and (c) are consistent with likely errors in the forcing functions. As already indicated the HR stresses may be too large due to the use of Bunker's (1976) drag coefficients and the heat fluxes in this region had smaller values in EK than in the other climatologies considered. The vertical thermal structure on the equator (fig.7b) also points to excessive upwelling.

The corresponding maps for September are shown in figs.6a and 6b. The simulation of SST for September has smaller differences from climatology than the simulation for March and this is evident from the feedback contribution to the surface heat flux in fig.6b. Note that the SSTs are too cold along the equator although, as pointed out earlier, this may be partly a consequence of the coarse resolution on which the climatological SSTs are defined. The main cause, however, is likely to be the surface

forcing. The temperatures in the west are simulated well by the model with the migration of the warm pool into the northern hemisphere in the northern summer.

The modelled equatorial SSTs around 120°W change very little from September to March and therefore the cold temperatures in March relative to climatology can be interpreted as a failure by the model to shut off, during the northern hemisphere spring, the mechanism responsible for the cooling. Both mooring data and climatological ship drift currents show a reversal of the surface currents near 120°W in late spring/early summer. The most likely cause of these anomalous currents is a surfacing of the equatorial undercurrent during a period of relaxed surface winds (Philander et al, 1987). The model does not produce strong surface current reversals at this time of year and this may be due to the temporal smoothing implicit in the use of monthly mean wind forcing. The mooring data shows the current reversal to be associated with a rise in the local SST. It is also associated with a decrease, or reversal, of the easterly wind which also, presumably, leads to a decrease in evaporation and hence heat loss by the ocean. Upwelling of colder water from below will also be reduced or cut-off. Cloud effects are also probably important in this region and to assess the relative importance of the various processes in producing the spring warming will only be possible in model simulations with improved flux datasets.

Turning next to the vertical thermal structure, fig. 7 shows the annual mean north - south temperature cross-section through 155°W from the Hawaii-to-Tahiti shuttle experiment (Wyrtki and Kilonsky, 1984) and from the model. Most features in the shuttle section are simulated by the model with the major differences occurring due to the excessive spreading of the thermocline above and below the undercurrent and the lack of ridging around 10°N. The thermocline spreading on the equator is clearly connected with the cold SSTs already discussed and from this temperature section the main cause again appears to be excessive upwelling. Two possible causes of the lack of doming at 10°N are an underestimation of the windstress curl by the HR winds and inadequate horizontal and vertical resolution in the ocean

model in the area of the NECC. These possibilities will be discussed further in the next two sections.

Fig. 7 also shows the mixed layer structure to be simulated well by the model in most areas. The near equatorial structure is viewed in another way in fig. 8, which shows the annual mean east-west temperature cross-sections from the model and the Levitus (1982) dataset at 2.5°N, equator and 2.5°S. After four years of integration the two off equator sections show that the model has generally kept the thermocline gradient whereas on the equator it has been spread out. The Levitus data is on a 1° grid and is a composite of all available XBT data so that the observed thermocline spreading will be somewhat smoothed. However, individual sections look more like the Levitus data than the model (Lemasson and Piton, 1968). Fig. 8 indicates that the structure of the modelled equatorial thermocline cannot be explained by a simple diffusion mechanism. The sreading is largely confined to the equatorial zone whereas the diffusion acts at all latitudes and the spreading is more likely associated with the vertical profile of the upwelling velocity. In the model simulation the vertical velocity profile in the central-west Pacific is parabolic in shape in that the velocity is zero at the surface (at the rigid lid) and zero below the undercurrent core, with a maximum around 40m so that the maximum vertical velocity is considerably above the main thermal gradient. This velocity profile acts to cause spreading of the isotherms in the upper part of the thermocline. The precise details of the profile are going to be dependent on a number of factors such as the mixing parametrization and the wind stress at the surface. Indeed, simulations with an Indian ocean version of the model, in which there is downwelling on the equator, has a thermocline which is too sharp.

The currents derived from the shuttle section are shown in fig. 9a (Wyrtki and Kilonsky, 1984). The model currents along the same section are given in fig. 9b. The core speed of the undercurrent is 90 cms-1 in both the data and the model. Shears below the undercurrent in the model are too weak but the vertical resolution is rather coarse at these depths. The meridional structure of the undercurrent is similar in both sections. In the shuttle data the NECC has a subsurface maximum of 40cms-1 whereas the model maximum

is only 20 cms-1, a result consistent with the lack of doming at 10°N in the model thermocline. In the data the North Equatorial Current (NEC) extends fairly deep into the ocean but in the model is essentially a surface Ekman drift. The lack of a significant sub-surface geostrophic NEC in the model is also associated with the small meridional thermocline gradients north of the dome.

5. RESULTS WITH MODELLED FORCING

From the end of the integration with climatological fluxes the model was integrated for a further 12 months using forcing fluxes from the atmospheric GCM. A subsequent four year integration (but with λ=100Wm-2K-1, see Gordon (1988)) showed that the characteristic features of the simulation in the upper ocean are present in this first year.

The SSTs for March are shown in fig. 10a and should be compared with figs. 1a and 4a. The extensive cold pool in the previous experiment has now disappeared and the SSTs are 2°C higher near 120°W on the equator. The model stresses are lighter in this region and there is a greater heat input into the ocean - both of these effects will tend to increase the temperature. The main errors in the simulation are now the 31°C water south of the equator in the west Pacific and the warm water between 28 - 29°C stretching across the Pacific at 5 - 7 degrees north of the equator. The 27°C isotherm on the equator does not extend so far west as in the previous experiment and the sharper tongue in fig. 9a is due to the increased temperatures north and south of the equator.

The increased heat input implied by the atmospheric GCM fluxes in the west accounts for the 31°C water in the southern hemisphere (Section 3). The AGCM heat flux in this region is within the current uncertainty in the observed heat flux estimates (Gordon, 1989). Oceanographic data indicates that the net surface heat flux in the west Pacific is small, being in the range 0 - 20Wm-2 (Godfrey and Lindstrom, 1989). The argument used by Godfrey et al is that both horizontal advection and diffusion of heat must be small. The former because horizontal gradients of temperature are weak

and the latter because vertical advection and entrainment of heat from below the mixed layer are also small. These vertical fluxes are small because the depth of the layer of active turbulence (the mixed layer, rather than the layer of near uniform temperature) is determined by the halocline gradients rather than the thermal profile and this depth is considerably less than the depth of near uniform temperatures. The temperature gradient at the mixed layer base is consequently small, so that the vertical advection and entrainment fluxes will also be small. This hypothesis is consistent with the model results presented here which suggest that the typical heat fluxes in the west Pacific from the EK climatology, shown in figs. 1c and 2c, lead to a better simulation of west Pacific SST than do the larger fluxes from the atmospheric model.

The warm water across the Pacific and north of the equator is caused by excessive heat advection by the NECC and by a local minimum in the evaporation associated with the low winds in the ITCZ. Surface current maps (not shown) show the NECC to be too strong across the width of the Pacific, which is a consequence of the wind stress curl pattern produced by the atmospheric GCM as discussed in Section 3. The too warm SSTs north of the equator in the west Pacific also mean that the water entering the NECC is too warm.

The SST field for September is shown in fig. 10b. The seasonal cycle in the east equatorial Pacific is simulated well. In the west the warm water follows the sun and in September is present both to the north and south of the equator. Along 7°S in the east Pacific the SSTs are 2 -3 °C warmer than climatology. The temperatures in this region were predicted well in the previous experiment and these errors with modelled forcing appear to be associated with the large heat input from the atmospheric GCM fluxes in this region (see fig. 4b). The major difference between the AGCM and EK heat fluxes in this region is the much larger value of the net surface shortwave flux from the model. Typical model values at 90°W between the equator and 15°S are around 250Wm-2, whereas the EK climatology suggests values around 160Wm-2. This discrepency is caused by an underestimation in the model of the low cloud associated with the cold SSTs extending away

from the South American coast . This indicates that the cloud distribution is of considerable importance in determining SST.

Temperatures along 5 - 7°N in September are even warmer than in March. On the equator the 27°C isotherm is in much the same position as it was in the first experiment. Comparing the zonal wind stresses for September (not shown) reveals that near 170°W the model stress is about 0.3 dyne/cm^2 which is larger than the climatological value (see figs. 2b and 4a). In addition the model heat flux in September (fig. 4b) has a local minimum of 20 Wm-2 near 170°W on the equator, and combined with the relatively large stress, this will lead to cold SSTs as shown in fig. 10b.

The September north - south temperature cross-section through 155°W is shown in fig. 11. The annual mean plot is not used because it will be biased by the fields at the initial time whereas by September the model has been integrated with AGCM fluxes for 12 months. It cannot be directly compared with the plots in fig. 7 but it is now clear that the thermocline doming near 10°N is far more pronounced than in the simulation with climatological fluxes and the NECC is consequently too strong. Also note the warm 29°C surface waters in fig. 11 above the main thermocline gradient, which are due to eastward advection by the NECC and low surface evaporation rates under the ITCZ.

Comparison of the undercurrent simulations for September at 155°W (fig. 12) shows the current to be weaker in the experiment with AGCM forcing than that obtained with climatological forcing. The core speed in the first experiment is 90cms-1, whereas in the simulation with model fluxes it is only 50cms-1. This large reduction in core speed at 155°W is largely caused by a shift in the longitudinal location in the current maximum. In the first experiment the overall maximum is 100cms-1, situated at around 130°W, but in the second experiment it has shifted eastward to 120°W and reduced in strength to 80cms-1. Fig. 12a also shows the undercurrent core to be displaced south of the equator. An interesting feature is that the westward surface current on the equator is actually stronger in the simulation with weaker winds. In September at 155°W the zonal stresses from HR and the atmospheric GCM are 0.65 and 0.55 dyne/cm^2 respectively,

whereas the westward surface currents from the corresponding simulations are 60cms-1 and 90cms-1. This result emphasises the importance of the non-linear vertical advection of eastward momentum from the undercurrent in the determination of the surface equatorial current.

6. COMPARISON WITH OTHER MODEL SIMULATIONS

Two studies have recently been published which model the seasonal response of the tropical Pacific ocean to climatological heat flux and wind stress forcing (Philander et al 1987, Seager et al 1988). The model described by Philander et al is similar to that used in this study although it has a higher resolution over a larger area of the ocean. In particular, there is higher resolution immediately below the mixed layer (10m resolution down to 100m) and also a 33km meridional resolution from 10°N to 10°S. The zonal resolution is 100km. The Philander et al model and that described here in Section 4 were forced with the seasonally varying HR wind stress climatology, although the formulation for the surface heat flux was rather different and consequently the simulated SSTs cannot be compared directly. (See Philander and Seigel (1985) for typical SST fields from their model). Surface current simulations were also different in the two models. The Philander el al model has a large meridional component to the equatorial currents in the central Pacific and often has current speeds near 1ms-1. In our study, equatorial currents were more down wind (i.e. zonal) with maximum speeds typically 80cms-1. This is probably due to greater momentum mixing in our model associated with the different buoyancy (heat) flux used.

It is useful to compare the subsurface thermal and current structure in the two models since this is primarily forced by the wind stress and wind stress curl which is the same i9n both. It was noted in Section 4 that our model underestimated the doming of the thermocline near 10°N and consequently the simulated NECC was too weak. However, Philander et al obtained a reasonable doming and NECC in their model forced with HR winds.

(Fig. 6 of their paper). This suggests that the coarser resolution in our model in the region of the NECC is responsible for the too weak current. In this region our model has roughly a 66km meridional grid spacing and Philander et al have 33km. The higher vertical resolution in their model may also be important since the region is one of large vertical thermal gradients. The equatorial undercurrent is also 10-20% stronger in the Philander et al simulation which is also most likely a consequence of the finer vertical resolution in their model in the region of the undercurrent.

In the study of Seager et al (1988) the model used is considerably different to the GCM used here. It is a version of the Zebiak and Cane (1987) 1½ layer model but modified to simulate total SST. There is an explicit treatment of a fixed depth upper Ekman layer while advection, mixing and local heating at the surface are all treated explicitly in the thermodynamic equation. In common with our formulation the short-wave flux has geographical variations associated with cloud and temporal variations were also included in some experiments. The latent heat flux is calculated via the standard bulk formulae assuming the 10m humidity mixing ratio is a constant fraction of the saturated humidity mixing ratio calculated at the SST. This approach gives a Haney coefficient (i.e. $\partial Q/\partial T$, see Section 2) which is considerably lower than the 35Wm-2K-1 used in the simulations described in this paper and so a direct comparison of SST is not possible. In addition different wind stresses were used in the two models (Seager et al used Rasmusson and Carpenter's (1982) wind climatology). However, it is interesting that whereas the GCM appears to overestimate the equatorial upwelling and therefore has a too extensive cold tongue the simpler model of Seager et al underestimates the cooling in the equatorial east Pacific. This may be partly due to the different wind stress used in the two simulations but may also be caused by model difficiencies unique to each of the models. The Seager et al model also has a rather poorly positioned warm pool, especially in the northern hemisphere summer whereas the GCM simulates this fairly well. Since local processes dominate in this region the major additional process in the GCM leading to the improved SST is the seasonal variation in mixed layer depth arising from the K-theory mixing scheme. A detailed comparison between simple models and GCMs both using the same forcing would be useful.

7. SUMMARY AND DISCUSSION

Two simulations have been performed to assess the sensitivity of a GCM of the tropical Pacific ocean to the specification of the surface forcing fluxes. The first set of forcing fields was taken from climatology and the second set from a multi-year integration of an atmospheric GCM. The latter set of fluxes is realistic in that the fluxes are generally within the bounds of uncertainty set by the various observational estimates.

When integrated with climatological fluxes the seasonal cycle of SST is reproduced well except during the period of weak SE trades in the east Pacific where SSTs are 2 - 3°C too cold. When the SE trades are at a maximum the SST is generally simulated better although there is excessive equatorial upwelling. The seasonal movements of the warm pool in the west Pacific are realistically modelled. Away from the equatorial region the vertical thermocline gradient is close to that observed whereas on the equator the model thermocline is too diffuse. The thermocline doming near 10°N is underestimated and the NECC is consequently too weak as is the geostrophic part of the NEC.

When integrated with atmospheric model fluxes the simulation changed considerably. The east Pacific was simulated reasonably well throughout the year but the west Pacific became too warm with temperatures rising to 31°C, mainly in regions of low level atmospheric convergence and therefore low winds. The main convergence region in the west has a strong seasonal signal and the warm water follows the convergence region throughout the year. Comparison with the first experiment indicates that heat fluxes in the range 0 - 20Wm^{-2} are required by this model to properly simulate the warm pool. The doming of the thermocline at 10°N and the NECC are both too strong as a result of the atmospheric model winds giving rise to too large wind curls north of the ITCZ.

It has been demonstrated that when two flux datasets, both realistic, are used to drive a GCM ocean model the resultant simulation of the seasonally evolving ocean state can be quite different in the two cases. The model shows considerable sensitivity to the specification of the surface fluxes, both of heat and momentum, and the experiments described in this paper indicate that improved climatologies of these fluxes are required.

REFERENCES

Bjerknes, J. (1966) A possible response of the atmopheric Hadley circulation to equatorial anomalies of ocean temperature. Tellus, 18, 820-829.

Bunker, A.F. (1976) Computations of surface energy flux and annual air-sea interaction cycles of the North Atlantic Ocean. Mon. Wea. Rev., 104, 1122 1140.

Cooper, N.S. (1988) The effect of salinity on tropical ocean models. J. Phys. Oceanog., 18, 697-707.

Cox, M.D. (1984) A primitive equation, 3-dimensional model of the ocean, GFDL Ocean Group Technical Report No.1, GFDL/NOAA, Princeton, N.J.

Enfield, D.B. (1986) Zonal and seasonal variability of the equatorial Pacific heat balance. J. Phys. Oceanog., 16, 1038-1054.

Esbensen, S.K. and Y. Kushnir (1981) The heat budget of the global ocean: An atlas based on estimates from surface marine observations. Report No.29, Climate Research Institute, Oregon State University, Corvallis.

Godfrey, J.S. and E. Lindstrom (1989) On the heat budget of the equatorial west Pacific surface mixed layer (Submitted to JPO).

Gordon, C. (1986) The development of a coupled GCM suitable for modelling studies in TOGA. In proc. of Workshop on Comparison of Simulations by Numerical Models of the Sensitivity of the Atmospheric Circulation to SST Anomalies, NCAR, Boulder, 1985.

Gordon, C. (1988) Air-sea interaction in a coupled TOGA model. Proceedings of the WGNE workshop on modelling the sensitivity and variations of the ocean-atmosphere system, ECMWF, May 1988.

Gordon, C. (1989) Comparison of the surface fluxes in the tropical Pacific ocean derived from an atmospheric general circulation model and from climatology. Tropical Ocean-Atmosphere Newsletter. (To appear).

Grahame, N.S. (1984) Simulations of the seasonal cycle of SST using globally specified climatological data to force simple ocean models. Dynamical Climatology Technical Note 5, Meteorological Office, Bracknell.

Gregg, M.C., H. Peters, J.C. Wesson, N.S. Oakey and T.J. Stay (1985) Intensive measurements of turbulence and shear in the equatorial undercurrent. Nature, 318, 140-144.

Haney, R.L. (1971) Surface thermal boundary conditions for ocean circulation models. J. Phys. Oceanogr., 1, 241-248.

Harrison, P.E., W.S. Kessler and B.S. Giese (1988) Ocean circulation model hindcasts of the 1982-83 El Nino: Thermal variability along the ship of opportunity tracks. (Submitted to J. Phys. Oceanogr.)

Hellerman, S. and M. Rosenstein (1983) Normal monthly winds stress over the world ocean with error estimates. J. Phys. Oceanogr., 13, 1093-1104.

Jaeger, L. (1976) Monthly maps of precipitation for the world ocean. D. Wetterd., Ber.18, Nr.139, Offenbach.

Latif, M. (1987) Tropical ocean circulation experiments. J. Phys. Oceanogr., 17, 246-263.

Lemasson, L. and B. Piton (1968) Anomalie dynamique de la surface de la mer le long de L'equateur dans l'Ocean Pacifique. Cah. ORSTOM. Ser. Oceanogr., 6, 39-45.

Levitus, S. (1982) Climatological atlas of the world ocean. NOAA Prof. Paper.

Pacanowski, R. and S.G.H. Philander (1981) Parametrization of vertical mixing in numerical models of the tropical oceans. J. Phys. Oceanogr., 11, 1443-1451.

Paulson, C.A. and J.J. Simpson (1977) Irradiance measurements in the upper ocean. J. Phys. Oceanogr., 7, 952-956.

Philander, S.G.H, W.J. Hurlin and A.D. Seigel (1987) Simulation of the seasonal cycle of the tropical Pacific ocean. J. Phys. Oceanogr., 17, 1986-2002.

Philander, S.G.H. and A.D. Seigel (1985) Simulation of El Nino of 1982/83. In Coupled Ocean-Atmosphere Models. Ed. J.C.J. Nihoul, Elsevier, 1985.

Rasmusson, E.M. and T.H. Carpenter (1982) Variations in tropical sea surface temperature and surface wind fields associated with the Southern Oscillation/El Nino. Mon. Weath. Rev., 110, 354-384.

Reynolds, W.R. (1982) A monthly climatology of sea surface temperature. NOAA Technical Report NWS 31, U.S. Department of Commerce.

Seager, R., S.E. Zebiak and M.A. Cane (1988) A model of the tropical Pacific sea surface temperature climatology. J. Geophys. Res., 93, No.C2, 1265-1280.

Schopf, P.S. (1983) On equatorial waves and El Nino II: Effects of air-sea thermal coupling. J. Phys. Oceanogr., 13, 1878-1893.

Shea, D.J. (1986) Climatological Atlas 1950-1979. Surface air temperature, precipitation, sea-level pressure and sea-surface temperature (45°S - 90°N). NCAR Technical Note TN-269, NCAR, Boulder.

Shukla, J. and M. Blackmon (1986) Proceedings of the Workshop on Comparison of Simulations by Numerical Models of the Sensitivity of the Atmospheric Circulation to Sea-Surface Temperature Anomalies, NCAR, Boulder, December 1985, WCP-121.

Slingo, A., R.C. Wilderspin and R.N.B. Smith (1988) The effect of improved physical parametrizations on simulations of cloud and the earth's radiation budget. (Submitted to J. Geophys. Res.)

Taylor, R.C. (1973) An atlas of Pacific island rainfall. Hawaii Inst. Geophys. Data Rep. No.25, HIG-73-9, 175pp.

Weare, B.C., P.T. Strub and M.D. Samuel (1980) Marine climate atlas of the tropical Pacific ocean. Department of Land, Air and Water Resources, University of California, Davis, 147pp.

Wells, N.C. and S. King-Hele (1988) Parametrization of tropical ocean heat flux. (Unpublished report).

Wyrtki, K. and Kilonsky, B. (1984) Mean water and current structure during the Hawaii-to-Tahiti Shuttle Experiment. J. Phys. Oceanogr., 14, 242-254.

Zebiak, S.E. and M.A. Cane (1987) A model El Nino-Southern Oscillation. Mon. Weather Rev., 115, 2262-2278.

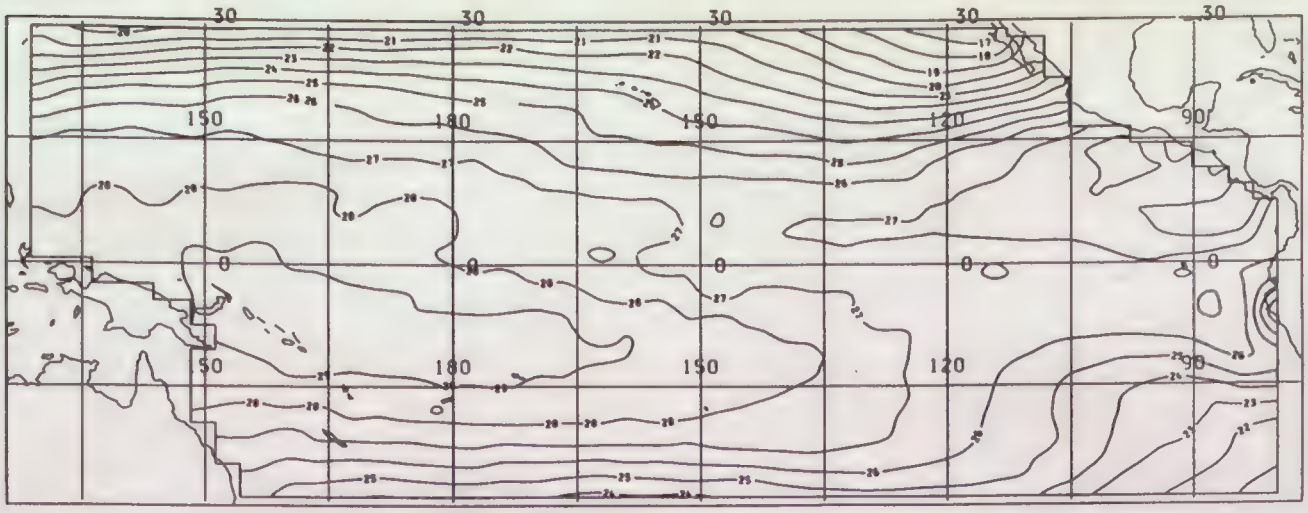

FIG.1(a) Climatological SST for March. The contour interval is 1°C. (UKMO Analysis).

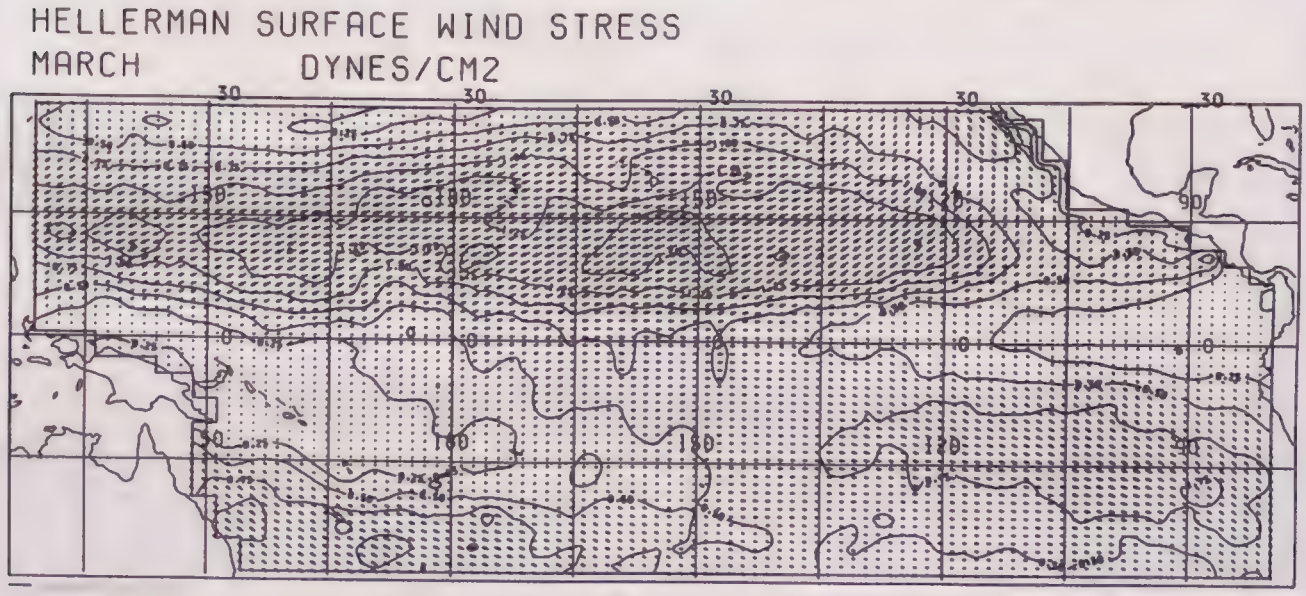

FIG.1 (b) Surface wind stress for March in dynes/cm^2. The contour interval is 0.25 dynes/cm^2. (Hellerman and Rosenstein).

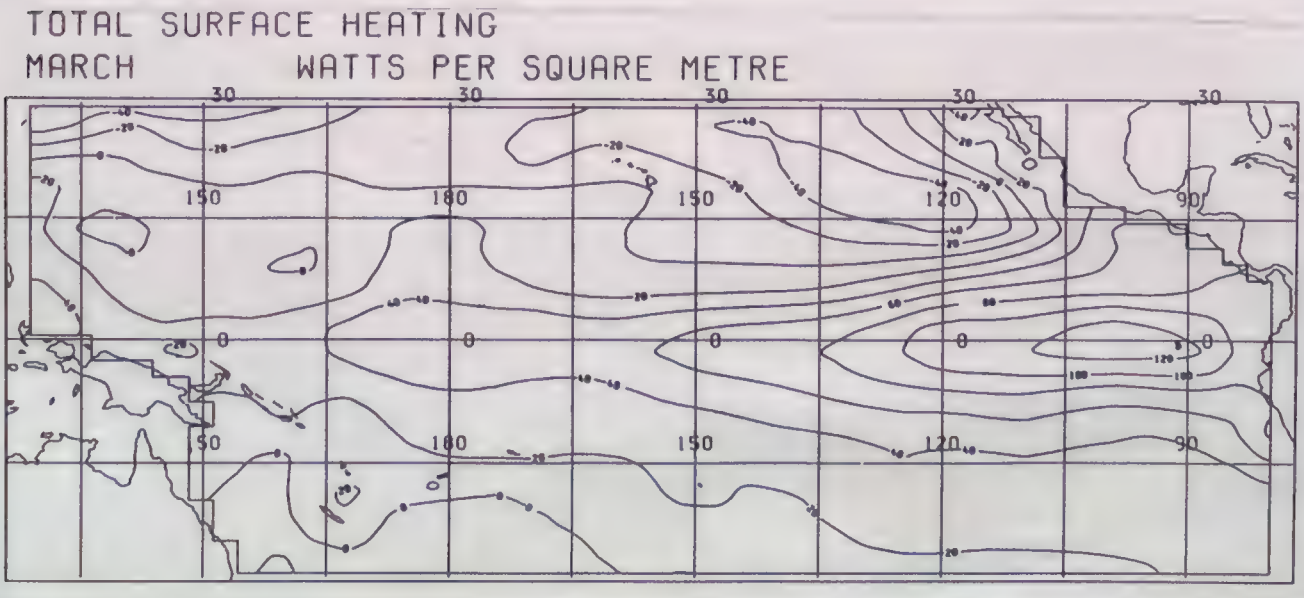

FIG.1(c) Total surface heat flux for March in Wm^{-2}. The contour interval is 20Wm^{-2}. (Esbensen and Kushnir).

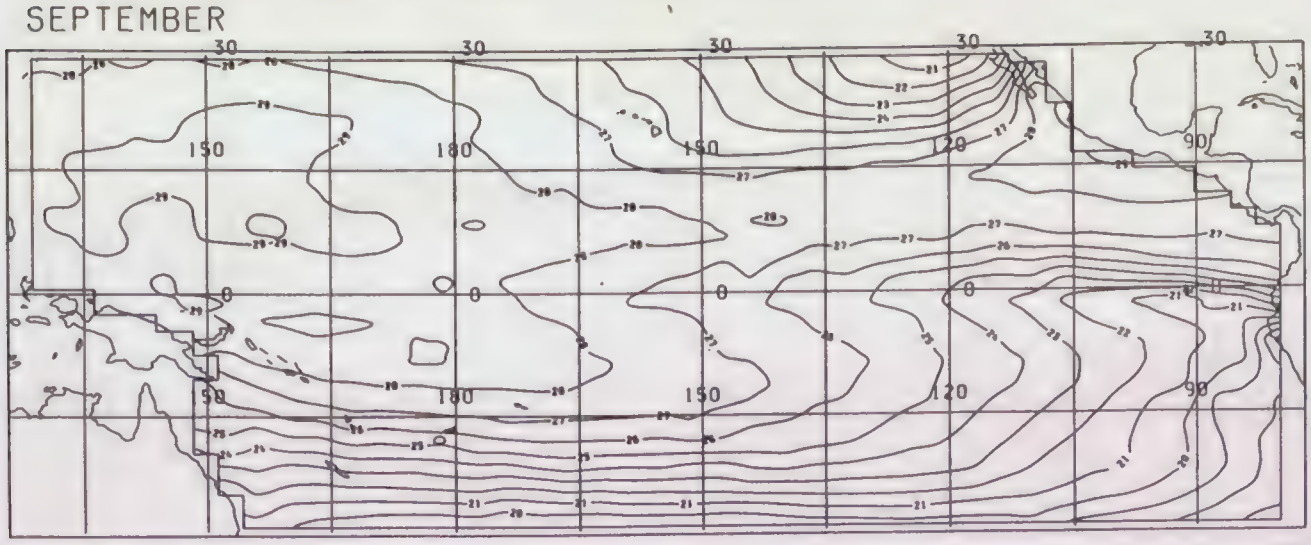

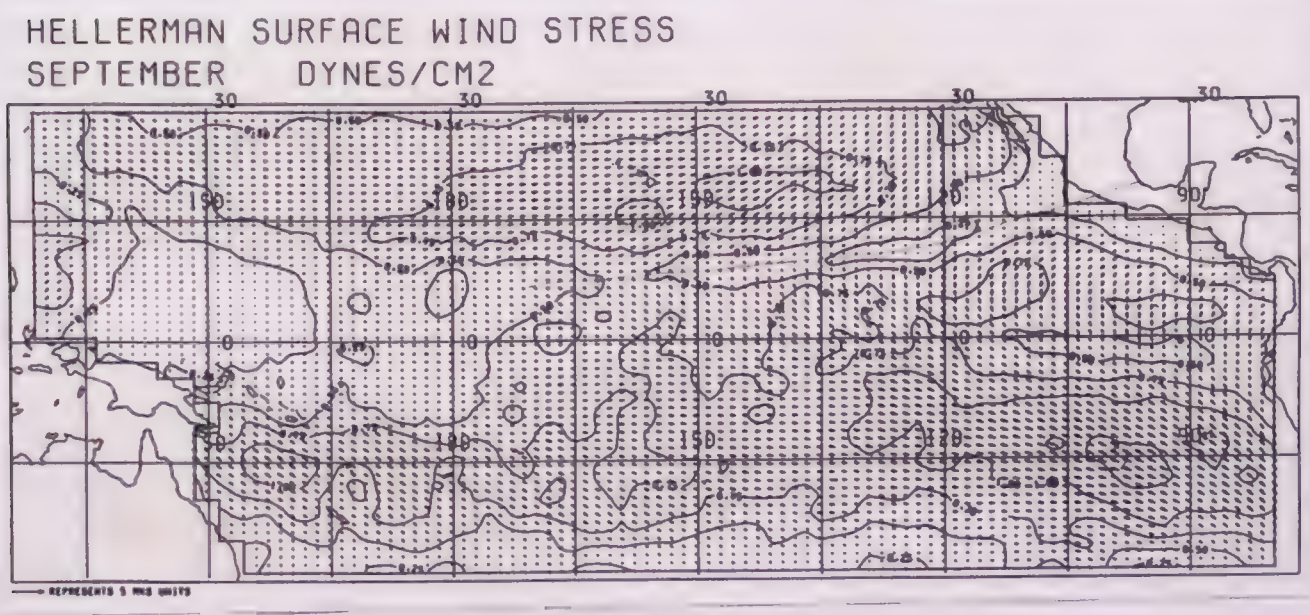

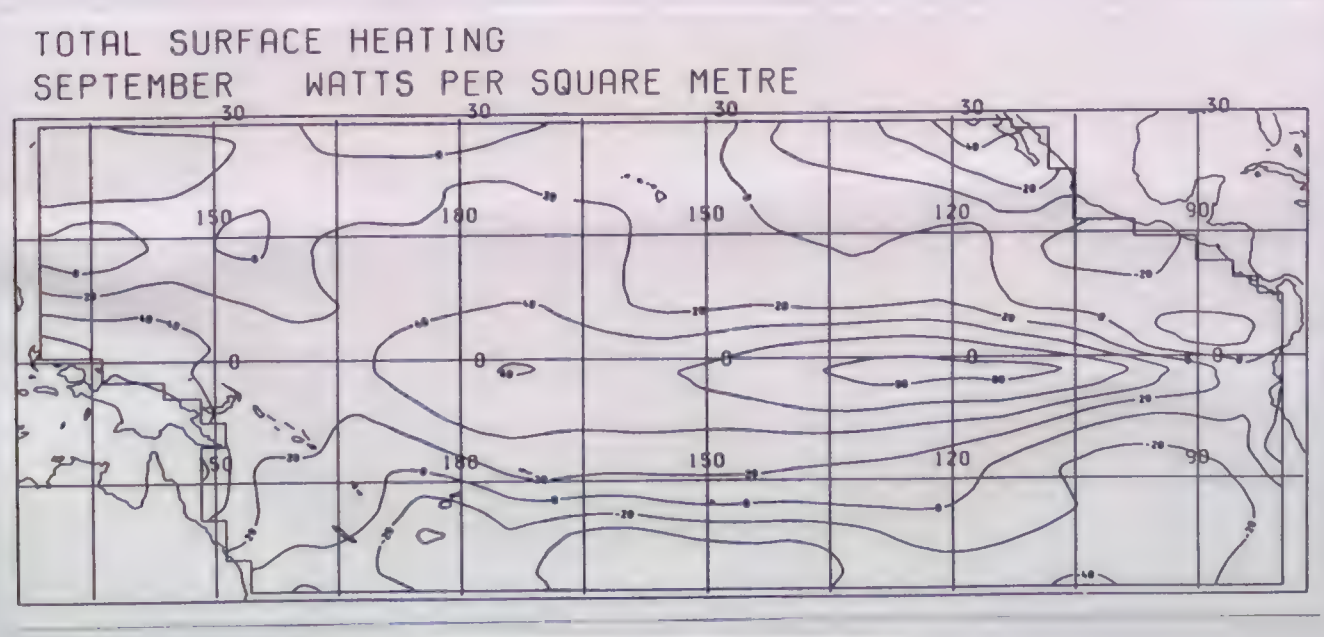

FIG.2: As fig.1 but for September.

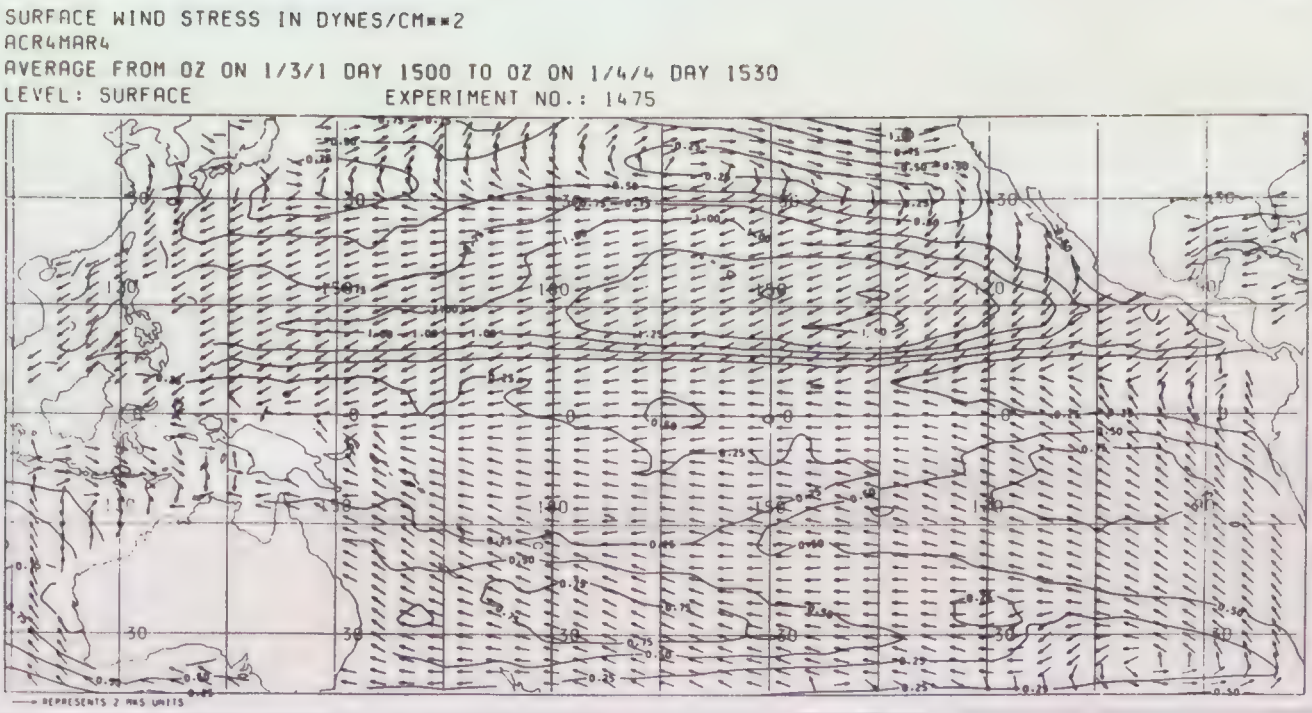

FIG.3(a) Average March surface wind stess from a 4-year integration of the atmospheric model.

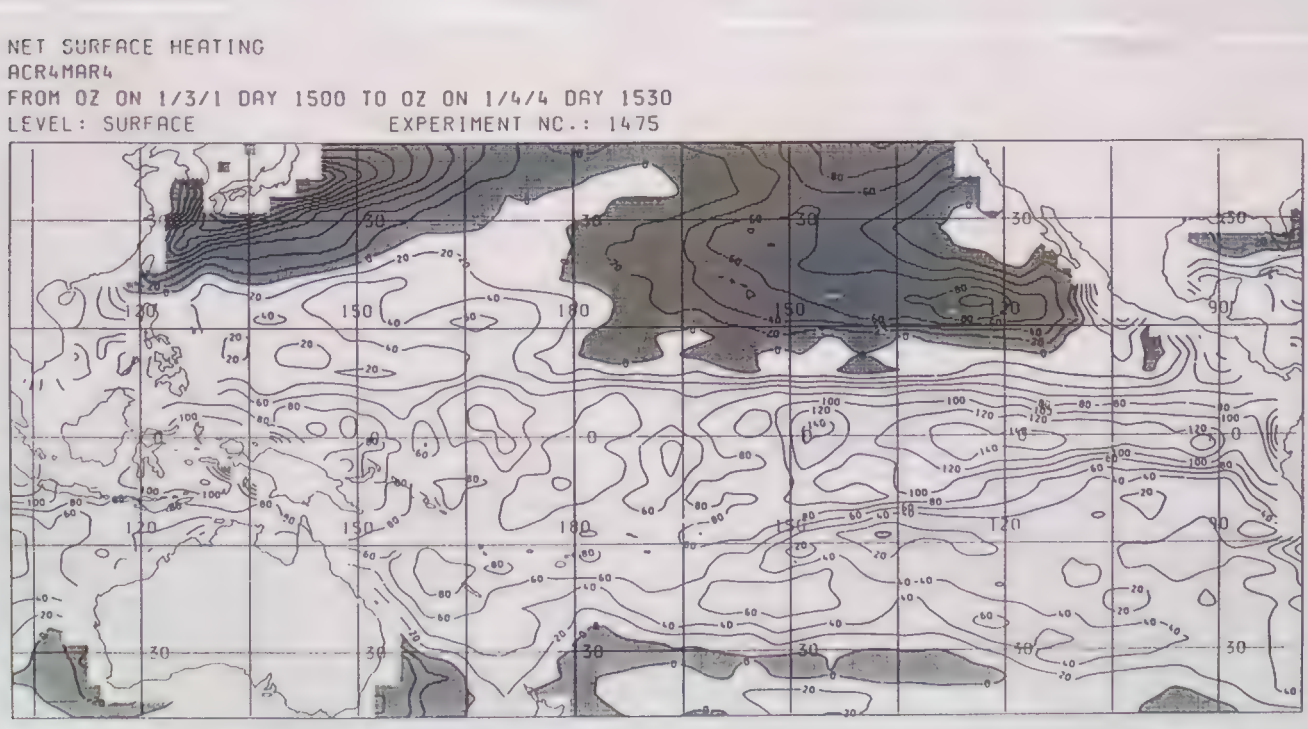

FIG.3(b) Average March net surface heat flux from a 4-year integration of the atmospheric model. (Contour intervals as in fig.1). Note that the latitudinal region covered is greater than that in fig.1.

SURFACE WIND STRESS IN DYNES/CM**2
ACR4SEP4
AVERAGE FROM 0Z ON 1/9 DAY 1320 TO 0Z ON 1/10/3 DAY 1350
LEVEL: SURFACE EXPERIMENT NO.: 1475

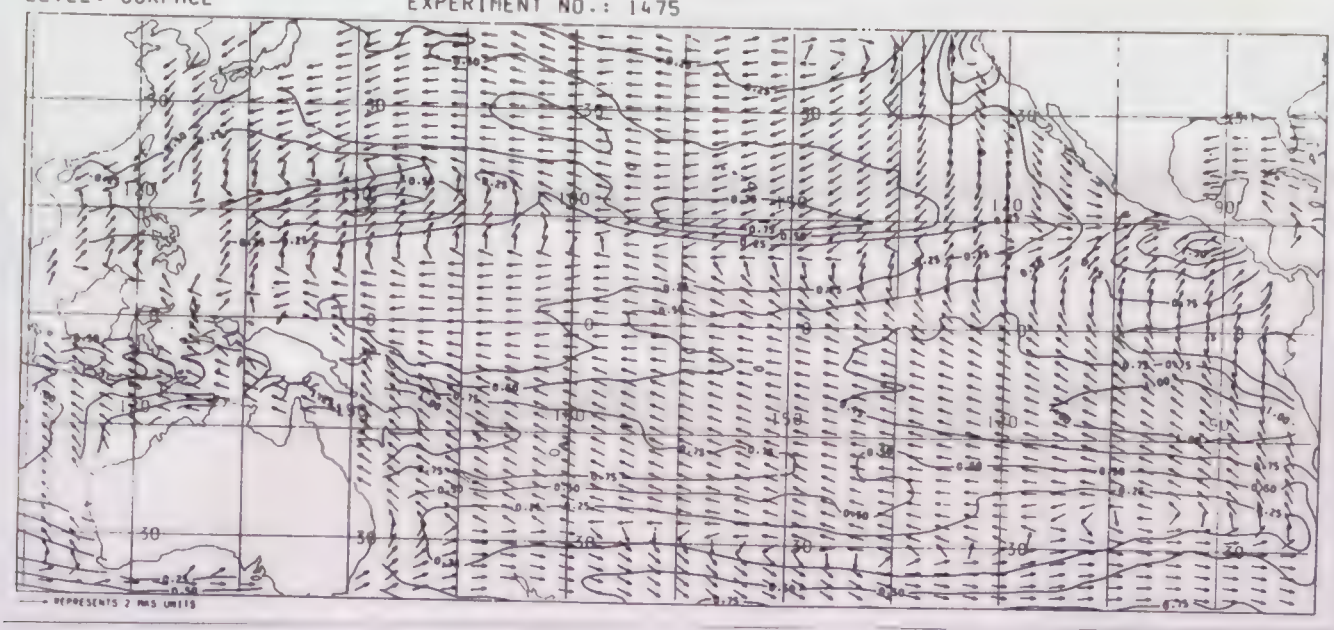

NET SURFACE HEATING
ACR4SEP4
FROM 0Z ON 1/9 DAY 1320 TO 0Z ON 1/10/3 DAY 1350
LEVEL: SURFACE EXPERIMENT NO.: 1475

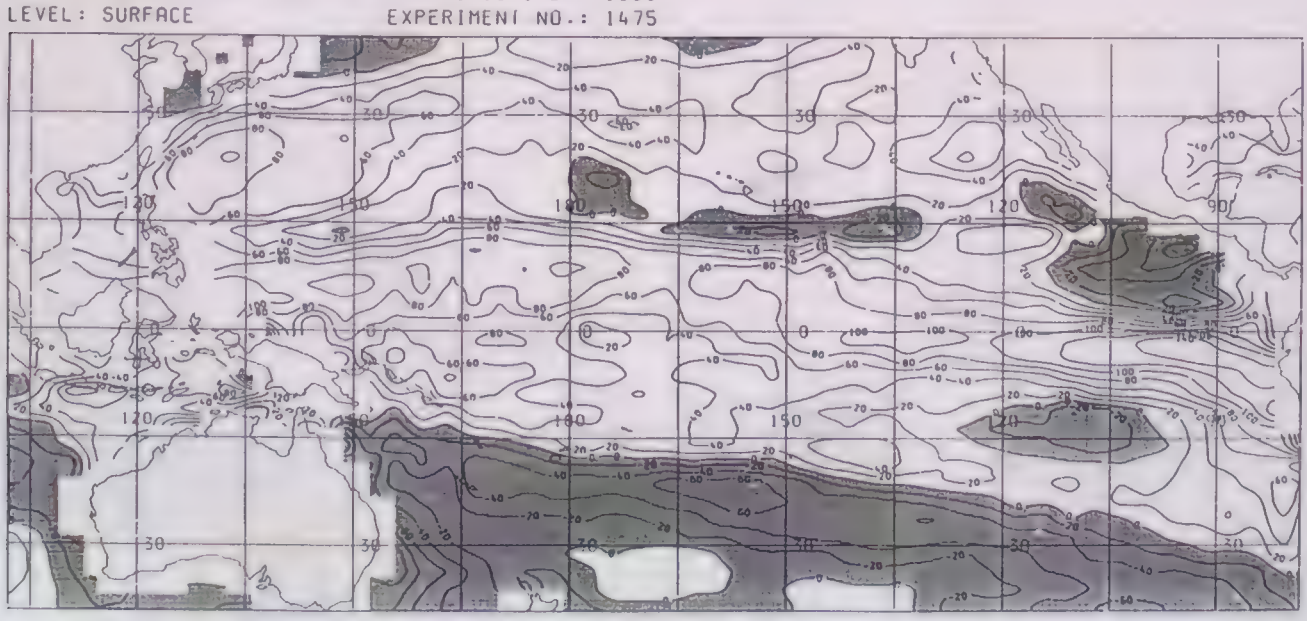

FIG.4: As fig.3 but for September.

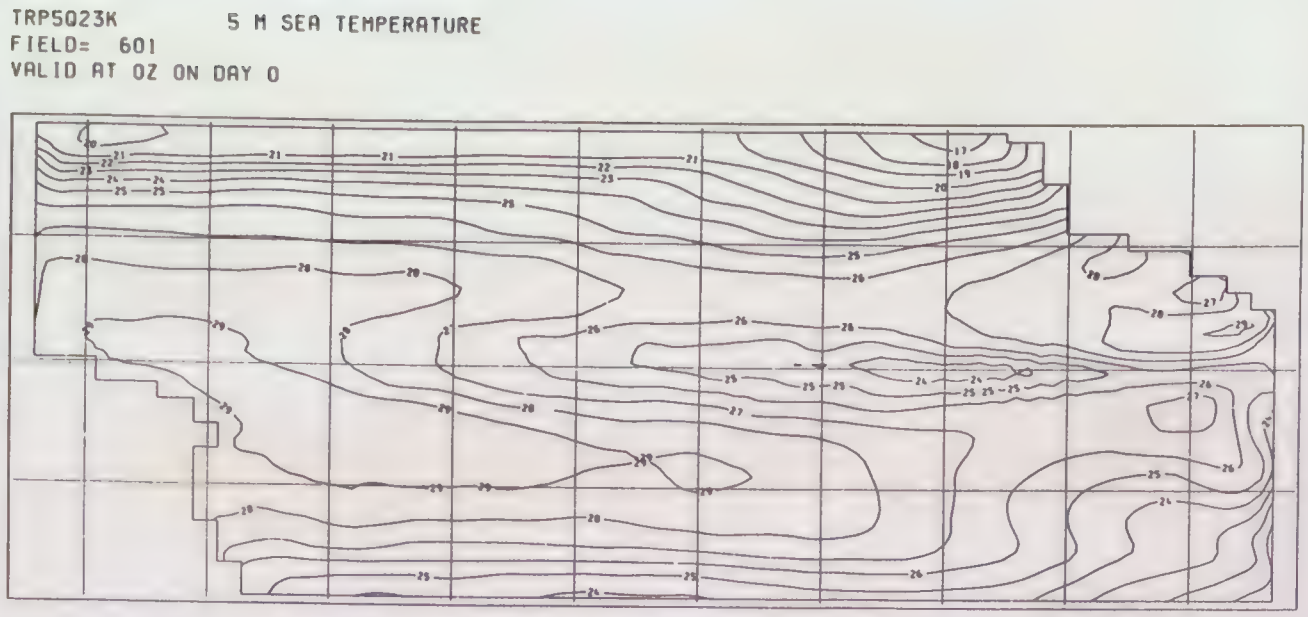

FIG.5: (a) The SST for March as simulated by the ocean model. In the west Pacific the SST compares well with climatology whereas the central east Pacific is too cold.

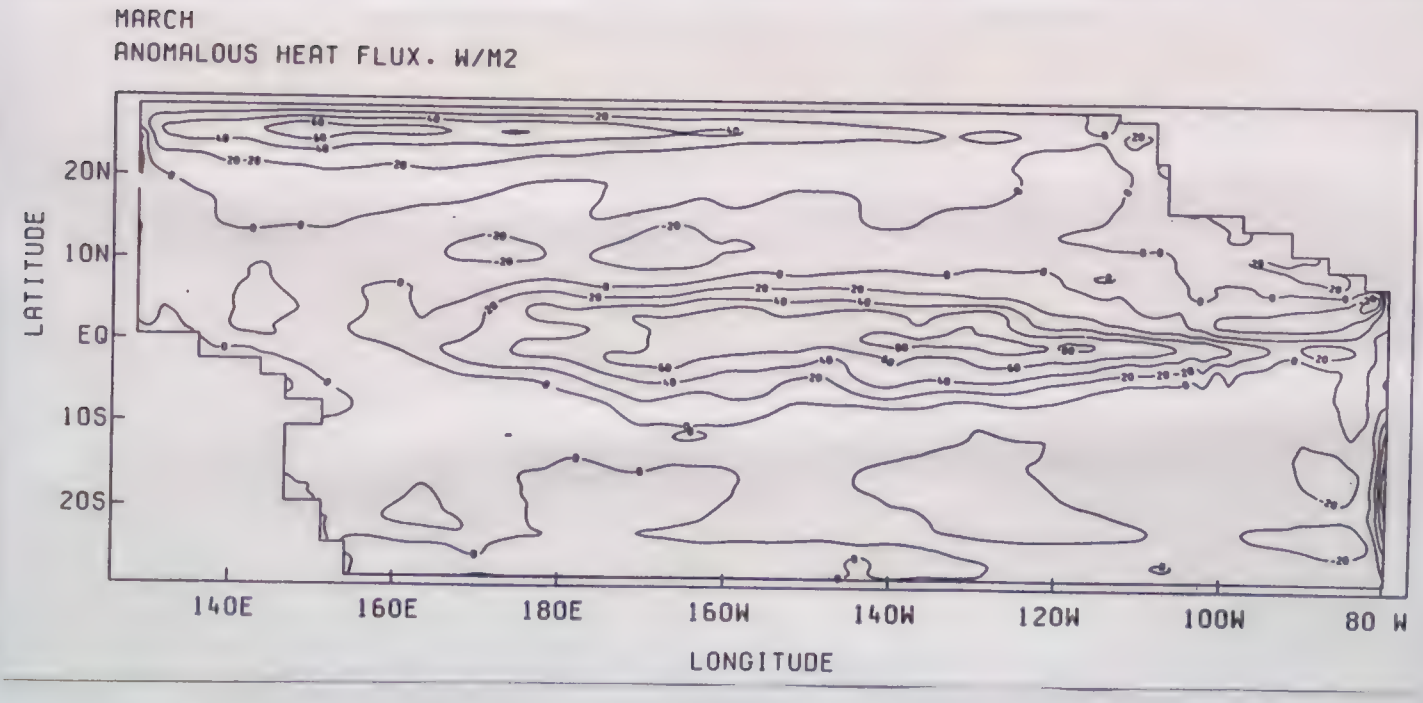

FIG.5(b) The contribution in March to the surface heat flux by the feedback term. The contour interval is 20Wm^{-2}. The maximum positive values over the warm pool are 80Wm-2.

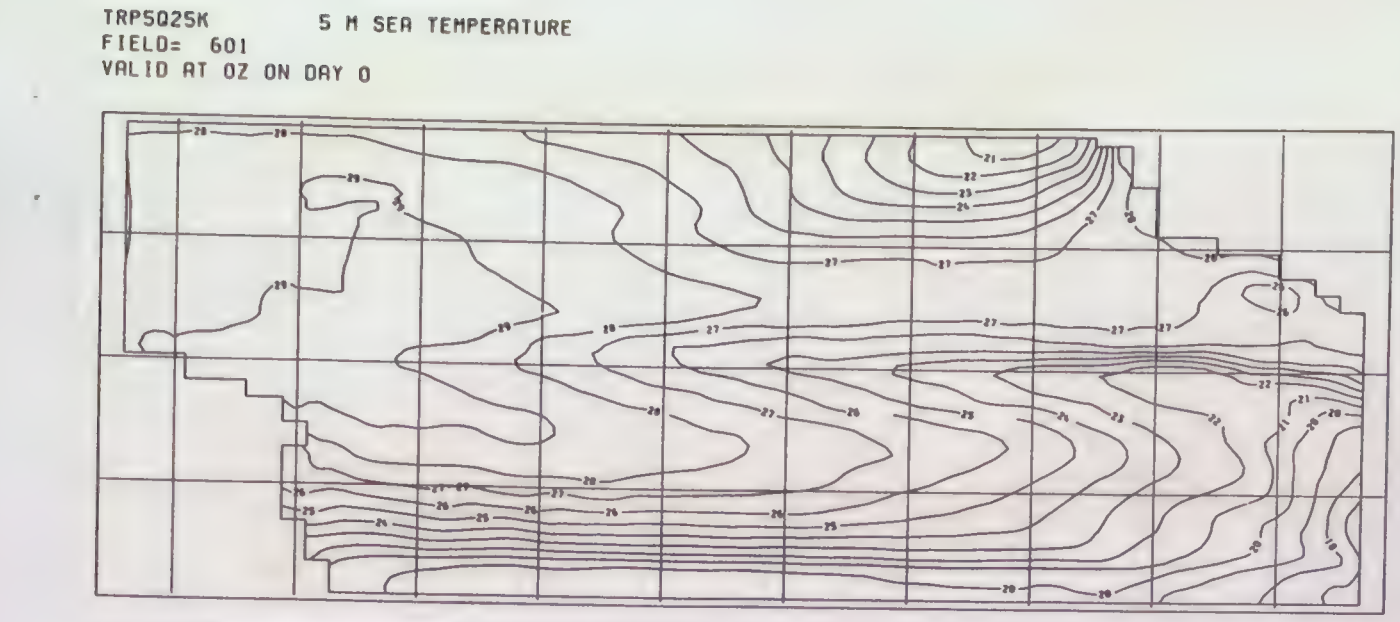

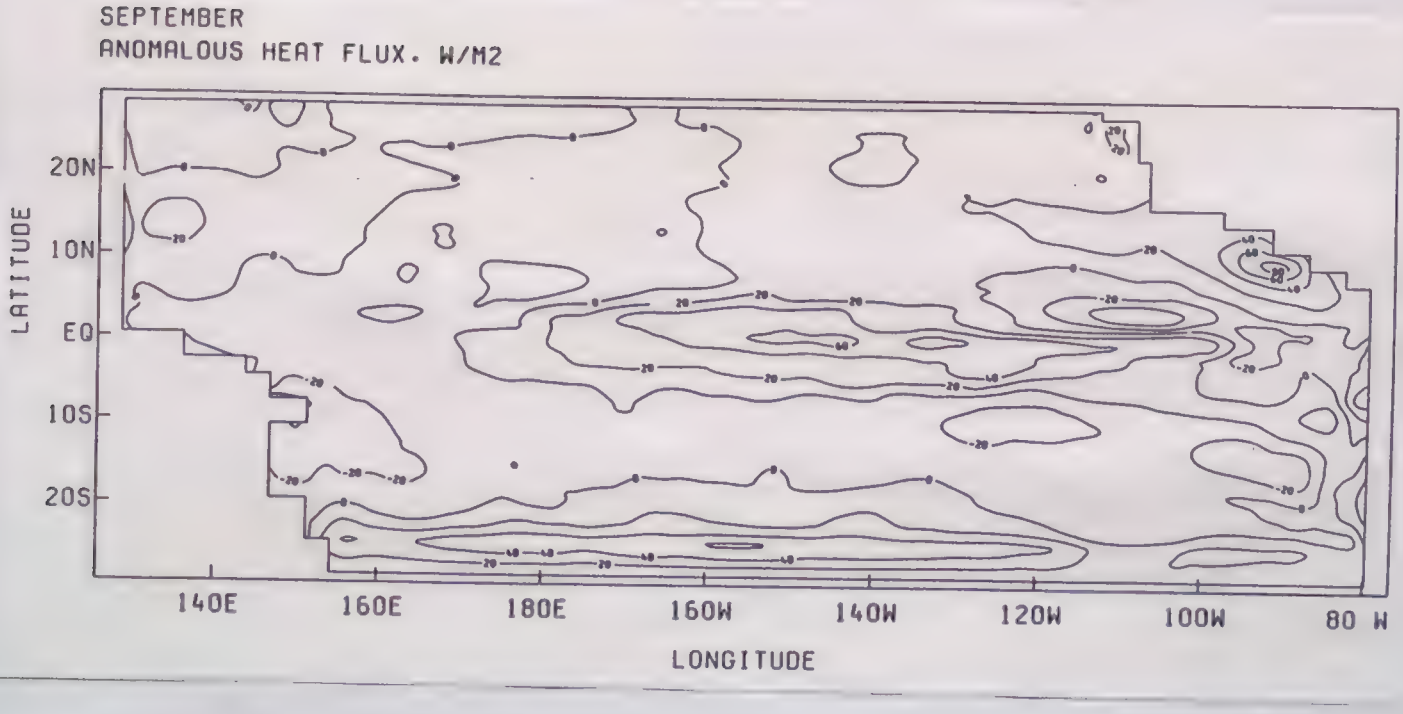

FIG.6: As fig.5 but for September. The SST are now reasonably well simulated in all areas. Maximum differences compared to climatology occur in the equatorial regions.

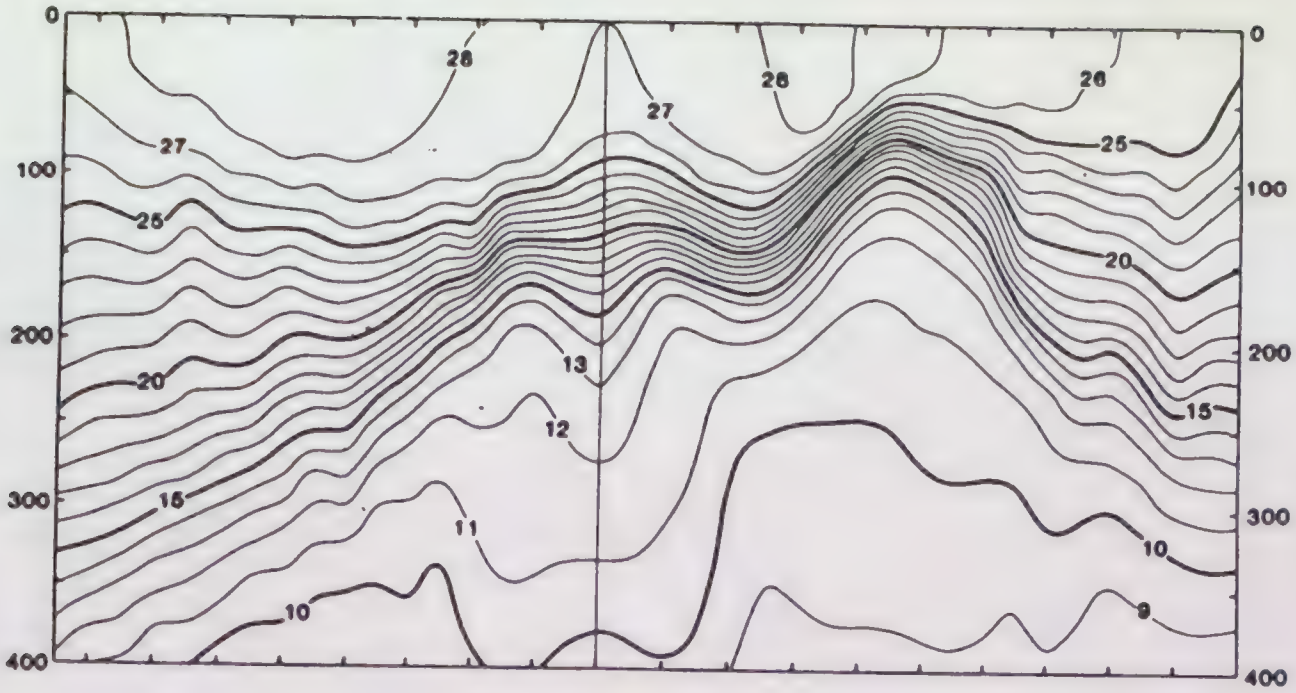

7(a)

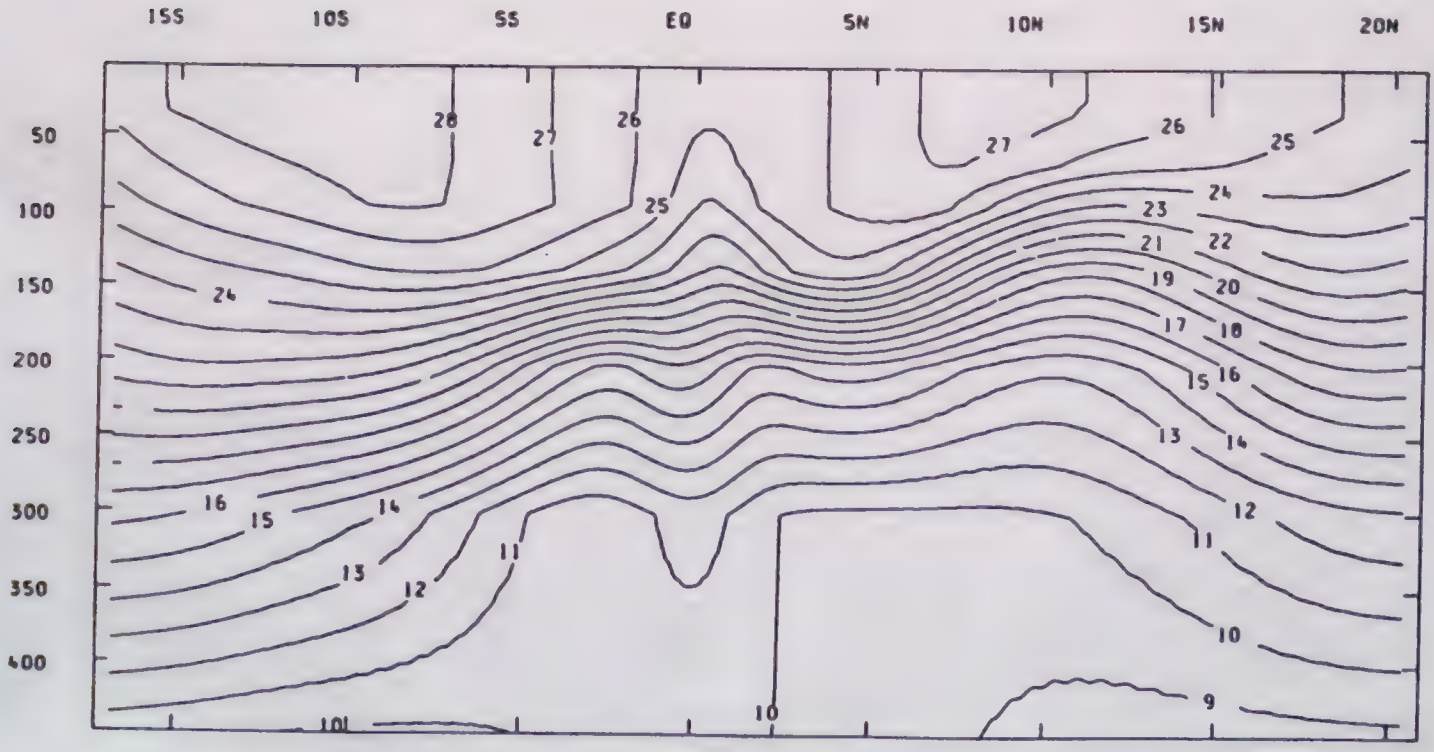

7(b)

FIGURE 7: North-South annual mean temperature section through 155°W from (a) the Hawaii-to-Tahiti shuttle and (b) the model. The major differences between the observed and modelled sections are the lack of doming near 10°N and the more diffuse thermal structure in the equatorial region in the model.

LEVITUS

MODEL

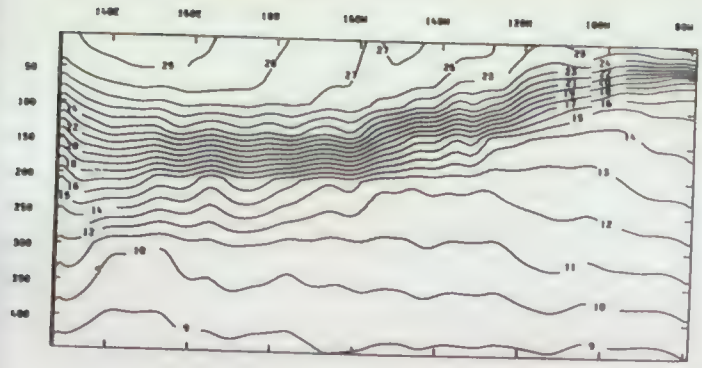

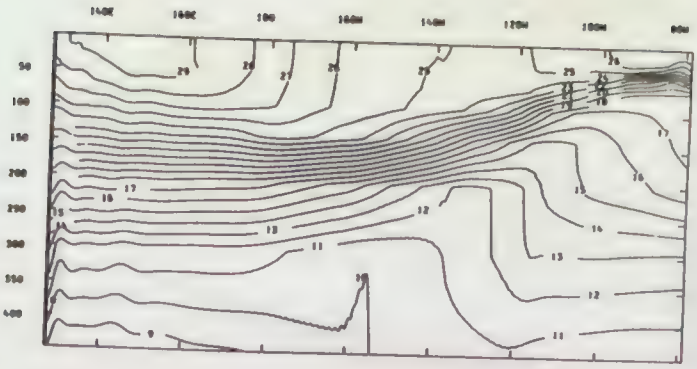

2.5°N

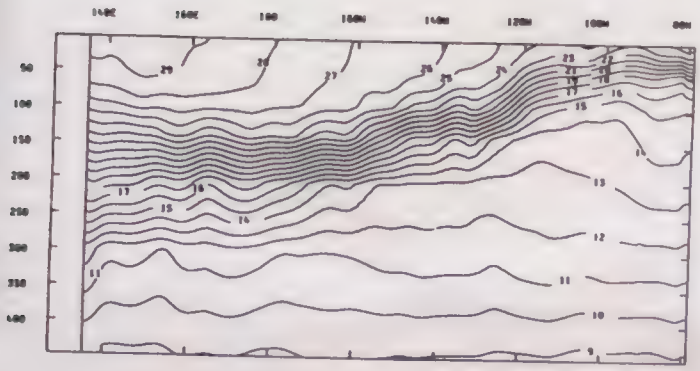

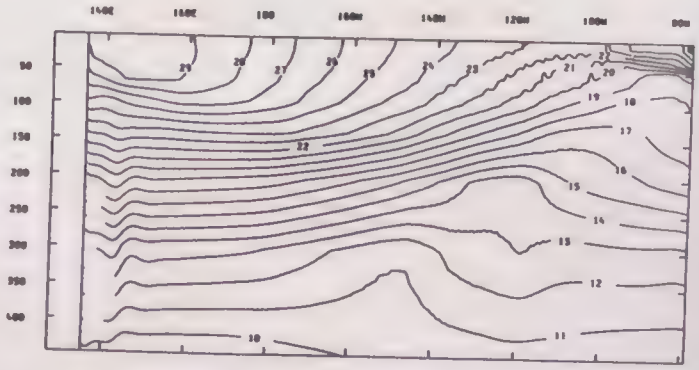

EQUATOR

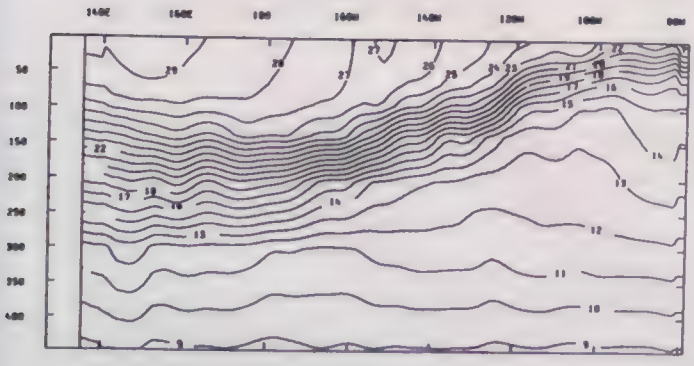

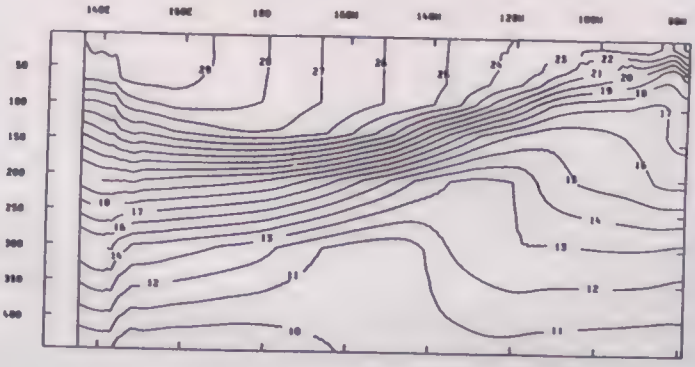

8(a) 2,5°S 8(b)

FIGURE 8: Annual mean longitude-depth temperature sections through 2.5°N, the equator and 2.5°S from (a) the Levitus (1982) climatology and (b) the model. The sharp gradients in the thermocline are simulated reasonably well north and south of the equator, however, right on the equator the thermocline is too diffuse.

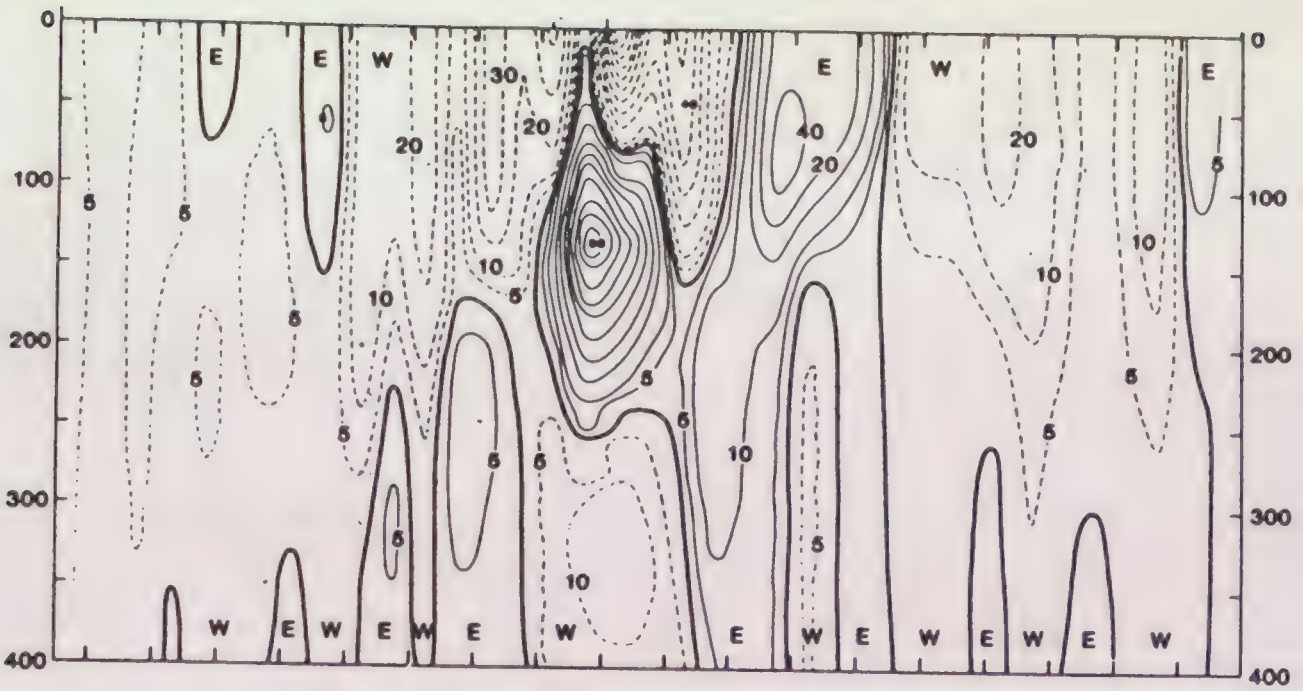

9(a)

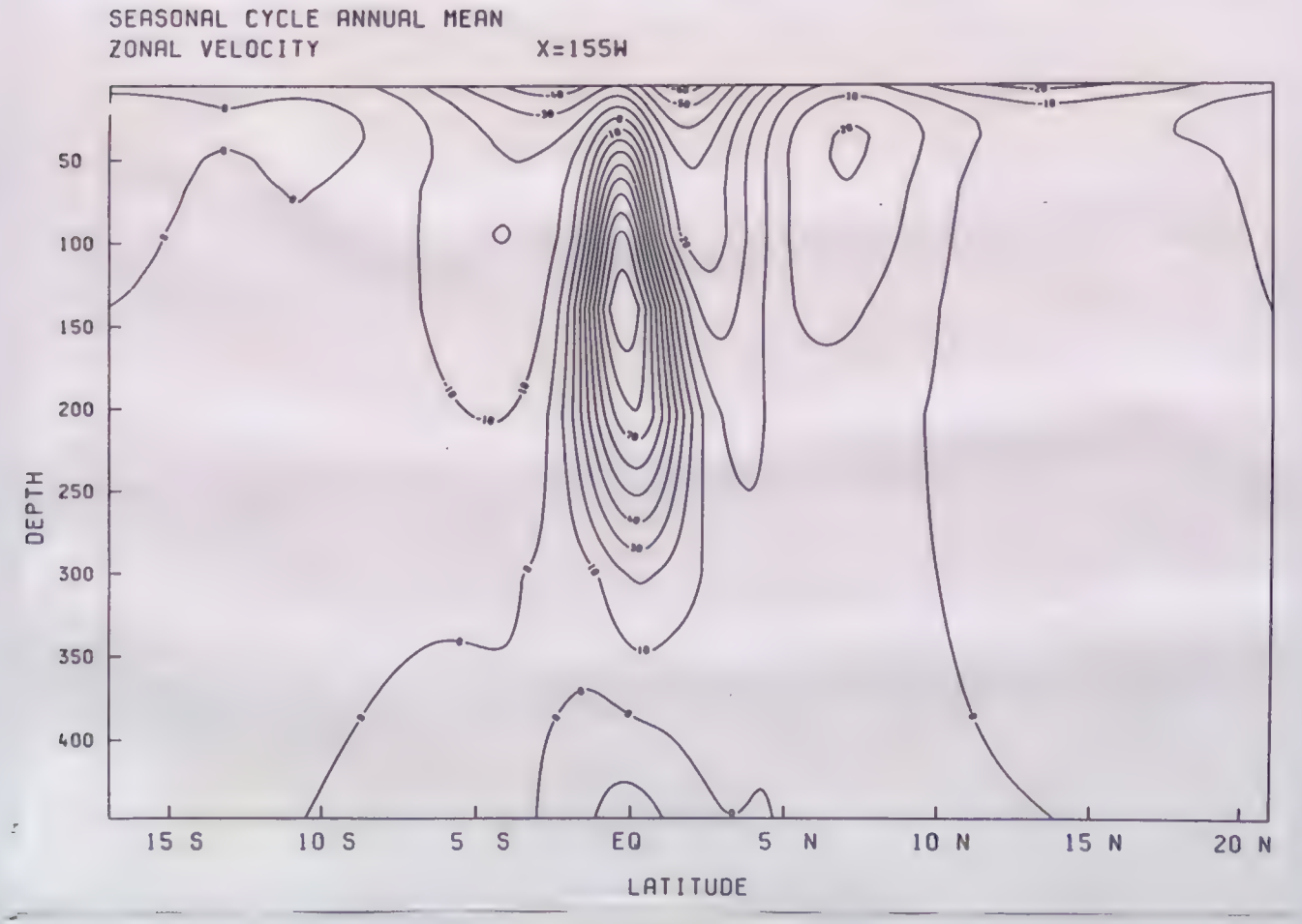

9(b)

FIG.9: Annual mean zonal current along 155°W as calculated (a) from the Hawaii-to-Tahiti shuttle data (Wyrtki and Kilonsky,1984) and (b) by the model. The depth and speed of the undercurrent is well simulated but the counter current and north equatorial current are too weak.

TRP7023K 5 M SEA TEMPERATURE
FIELD= 601
VALID AT 0Z ON DAY 0

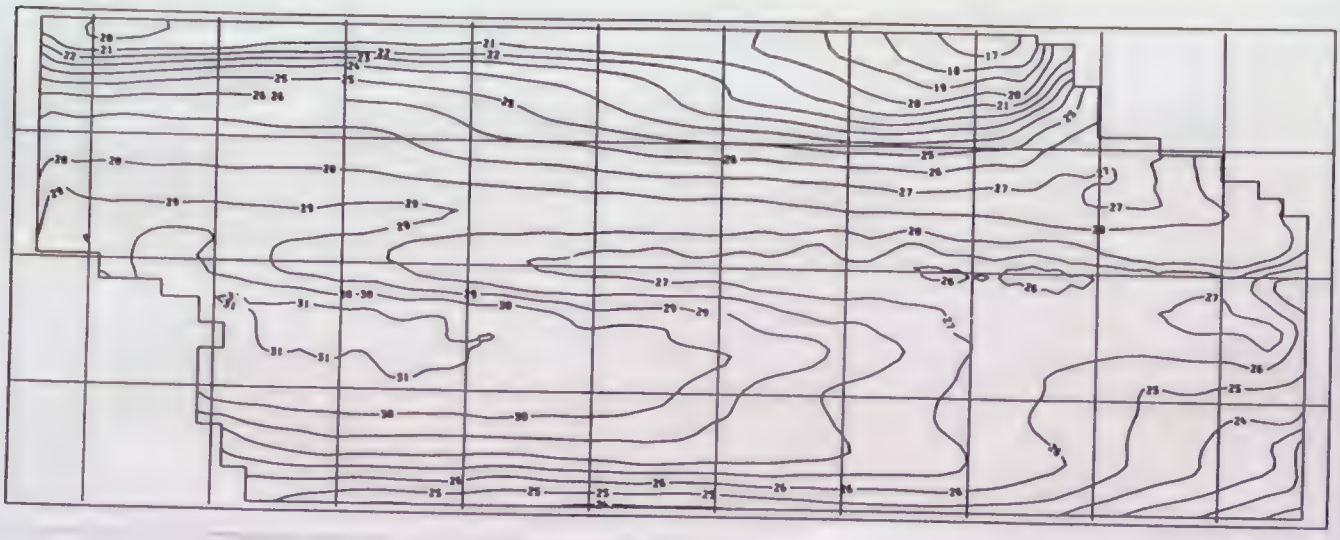

FIG.10(a) The modelled SSTs for March using AGCM fluxes.

TRP7025K 5 M SEA TEMPERATURE
FIELD= 601
VALID AT 0Z ON DAY 0

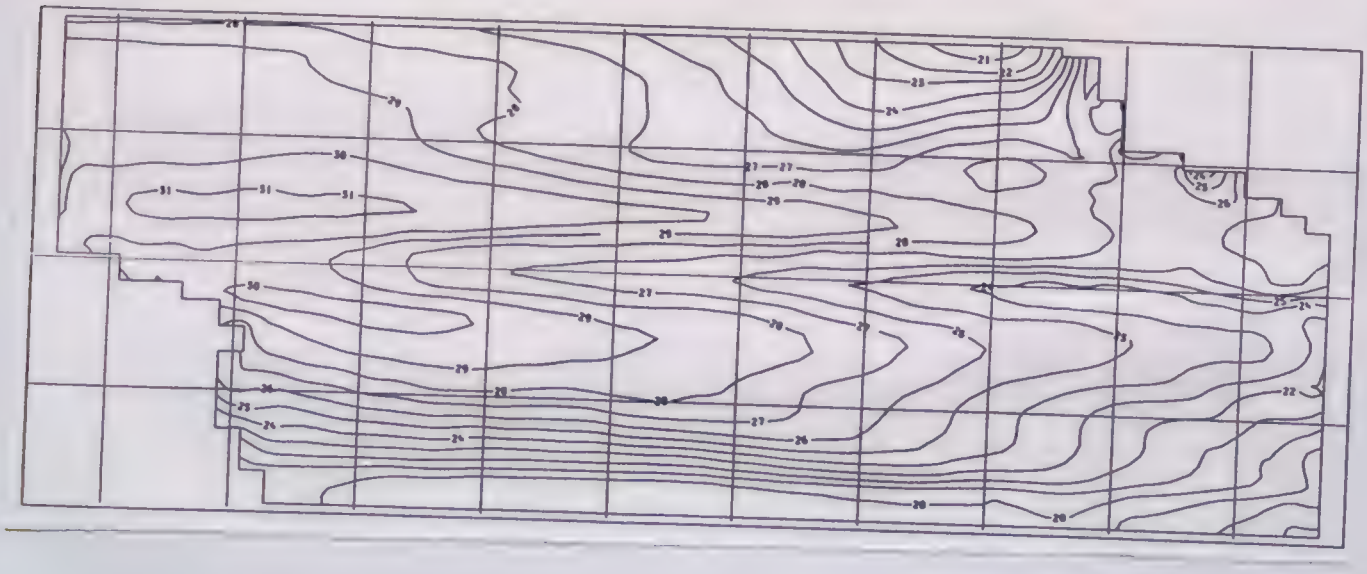

FIG.10(b) The modelled SSTs for September using AGCM fluxes. In March the SSTs in the warm pool region under the SPCZ are now too warm compared with climatology. In September, the too warm water is present both north and south of the equator in the west Pacific. The east Pacific is reasonably well simulated in both March and September.

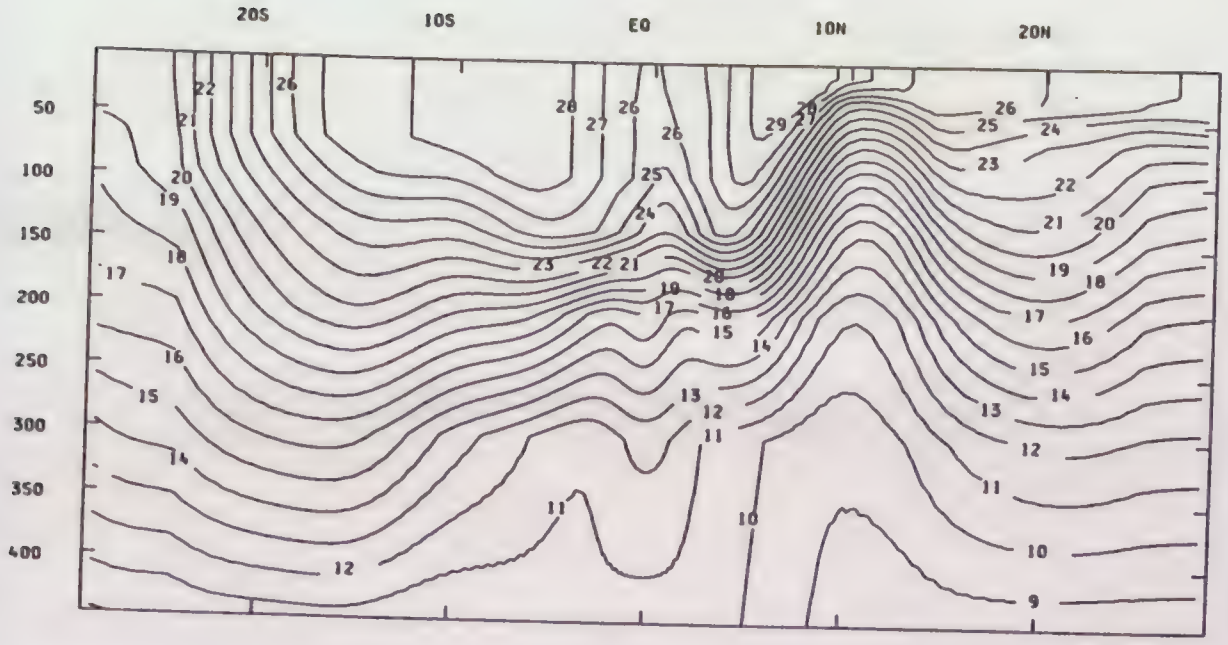

FIGURE 11: North-South cross section through 155°W for September from the model using atmospheric model fluxes. There is a much greater doming of the thermocline near 10°N than in the experimemt with climatological fluxes. (Note the latitudinal scale is different to that in fig.6)

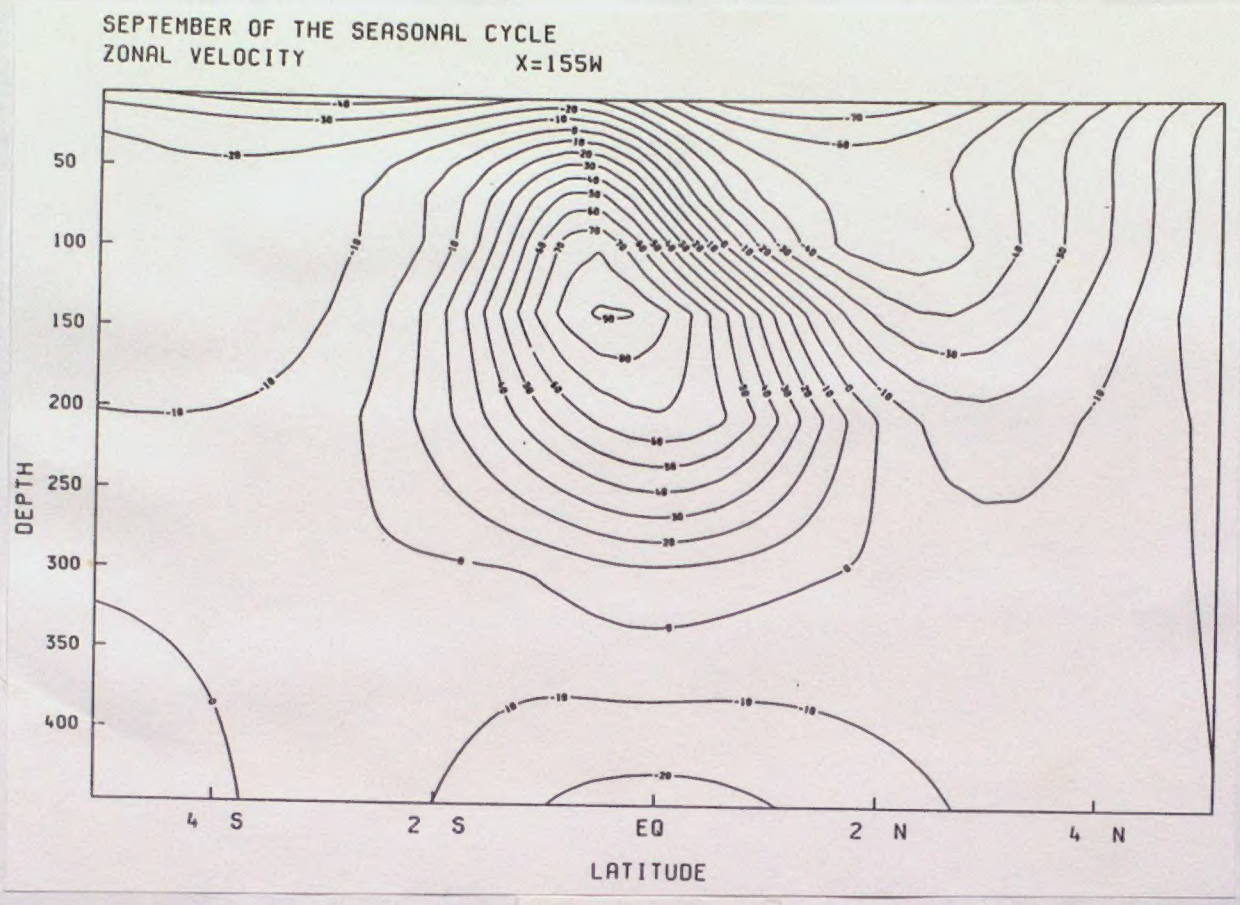

12(a)

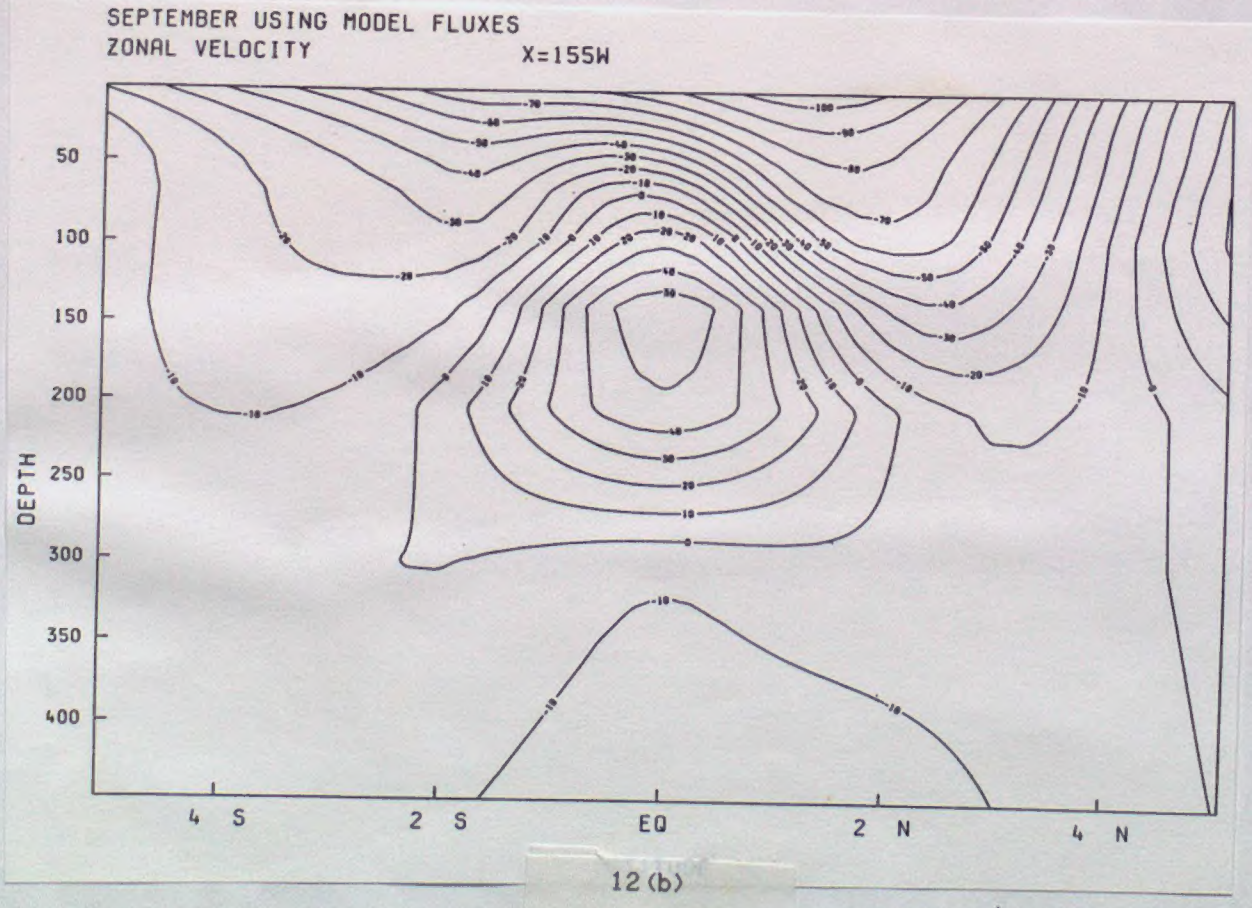

12(b)

FIGURE 12: The zonal velocity section through 155°W for September from the experiment with (a) climatological fluxes and (b) modelled fluxes.

DYNAMICAL CLIMATOLOGY TECHNICAL NOTES

DCTN 1	June 1984	A scheme for incorporating the thermodynamic sea-ice model into a coupled ocean-atmosphere model. C Gordon and M Bottomley
DCTN 2	Sept 1984	The parametrization of the upper ocean mixed layer in coupled ocean/atmosphere models. C Gordon and M Bottomley
DCTN 3	Sept 1984	The response of a simple thermodynamic sea-ice model to GCM forcing appropriate for perennial sea-ice. M Bottomley
DCTN 4	Sept 1984	Potential vorticity in the stratosphere derived using data from satellites. S A Clough, N S Grahame and A O'Neill
DCTN 5	Sept 1984	Simulation of the seasonal cycle of SST using globally specified climatological data to force simple ocean models. N S Grahame
DCTN 6	Sept 1984	Development of an improved GCM radiation scheme. A Slingo and R C Wilderspin
DCTN 7	Sept 1984	On the specification of surface fluxes in coupled atmosphere/ocean general circulation models. J F B Mitchell, C A Wilson and C M Price
DCTN 8	Sept 1984	A survey of possible repercussions of the Soviet river reversal programme on Arctic sea-ice. H Cattle
DCTN 9	Oct 1984	A study of a strong stratospheric warming during January 1982 T D A Fairlie
DCTN 10	Nov 1984	An intercomparison of the Met O 11 N45 model and the Met O 20 11-level model on the Cyber 205 J F Dyson
DCTN 11	Nov 1984	Simulation of observed time series of temperature and precipitation over eastern England. D N Reed
DCTN 12	Nov 1984	Forecasts and analyses of the onset of the Southwest monsoon. R Kershaw
DCTN 13	Nov 1984	On modelling the effects of CO_2 on climate. J F B Mitchell
DCTN 14	Dec 1984	Development of a revised longwave radiation scheme for an atmospheric general circulation model. A Slingo and R C Wilderspin
DCTN 15	Jan 1985	Rossby wavetrains in the stratosphere forced by localised disturbances in the troposphere. C J Marks (Oxford), A O'Neill and V D Pope

DYNAMICAL CLIMATOLOGY TECHNICAL NOTES

DCTN 16	Jan 1985	Observing system experiments using the Meteorological Office's 15-level model. R A Bromley
DCTN 17	Feb 1985	Atmospheric general circulation simulation of the climate of the Mediterranean region. H Cattle
DCTN 18	Feb 1985	Diurnal variation and cloud in a general circulation model. C A Wilson and J F B Mitchell
DCTN 19	Feb 1985	The sensitivity of the Saharan region in a general circulation model. W M Cunnington and P R Rowntree
DCTN 20	Mar 1985	The impact of aircraft observations on analyses and forecasts from the operational 15-level model. B R Barwell
DCTN 21	Mar 1985	Non-linear effects on heat-induced circulation of the tropical atmosphere. A E Gill and P J Phlips
DCTN 22	Apr 1985	Simulation of cloudiness with the U.K. Meteorological Office 11-layer AGCM. A Slingo and R C Wilderspin
DCTN 23	Apr 1985	An integrated approach to the representation of cloud processes. R N B Smith
DCTN 24	May 1985	Nuclear Winter: Calculations of the shortwave radiative effects of soot aerosols. A Slingo and P Goldsmith
DCTN 25	Jul 1985	Sea ice and the Antarctic winter circulation: a numerical experiment. J F B Mitchell and T S Hills
DCTN 26	Jul 1985	A Budyko-Sellers model for study of ocean-atmosphere interaction. W J Ingram
DCTN 27	Aug 1985	The effect of a shoaling thermocline on equatorially-trapped Kelvin waves. A E Gill and B A King
DCTN 28	Sept 1985	CO_2 climate sensitivity and model dependence of results. J F B Mitchell, C A Wilson and W M Cunnington
DCTN 29	Sept 1985	Handbook of the Meteorological Office 11-layer atmospheric general circulation model. Volume 1 : Model Description Edited by A Slingo
DCTN 30	Sept 1985	Impact of land surface variations on African rainfall in general circulation models. P R Rowntree, M F Wilson and A B Sangster

DYNAMICAL CLIMATOLOGY TECHNICAL NOTES

DCTN 31 Nov 1985 The annual cycle of sea level in the eastern tropical Pacific.
G R Bigg and A E Gill

DCTN 32 Nov 1985 An analytic model of the heat-induced tropical circulation in the presence of a mean wind.
P J Phlips and A E Gill

DCTN 33 Nov 1985 The effect of resolution and diffusion on the simulated climate.
J F Dyson

DCTN 34 Jan 1986 Rossby adjustment over a step.
M K Davey, A E Gill, E R Johnson and P F Linden

DCTN 35 Jan 1986 Issues concerning the evaluation of effective surface roughness of heterogeneous terrain.
D J Carson

DCTN 36 Mar 1986 Climate sensitivity and past climates : evidence from numerical studies
J F B Mitchell

DCTN 37 Mar 1986 Parametrizations of land-surface processes in Meteorological Office numerical weather prediction and climate models
D J Carson

DCTN 38 Apr 1986 Modelling of land-surface processes and their influence on European Climate
D A Warrilow, A B Sangster and A Slingo

DCTN 39 Apr 1986 Simulation of climatic change due to increased CO_2
J F B Mitchell

DCTN 40 May 1986 On the interpretation of the Eliassen-Palm flux divergence.
Part I : Theory
D G Andrews

DCTN 41 June 1986 Experiments on tropical circulation with a simple moist model.
M K Davey and A E Gill

DCTN 42 Jun 1986 Parameter regimes for studying isolated eddies.
P D Killworth and M K Davey

DCTN 43 Jun 1986 A comparison of the impact of an envelope orography and of a parametrization of orographic gravity-wave drag on model simulations.
A Slingo and D W Pearson

DCTN 44 Jul 1986 The effect of a sea-surface temperature anomaly on a prediction of the onset of the south-west monsoon over India.
R Kershaw

DCTN 45 Jul 1986 An introduction to the parametrization of land-surface processes.
D J Carson

DYNAMICAL CLIMATOLOGY TECHNICAL NOTES

DCTN 46 Sept 1986 Lateral boundaries and the heat-induced flow in the tropical atmosphere.
P J Phlips and A E Gill

DCTN 47 Nov 1986 Simulation of the diurnal cycle of outgoing longwave radiation with an atmospheric GCM.
A Slingo, R C Wilderspin and S J Brentnall

DCTN 48 Feb 1987 A 2 x CO_2 climate sensitivity experiment with a global climate model including a simple ocean
C A Wilson and J F B Mitchell

DCTN 49 Feb 1987 Sensitivity of the Met O 20 11-layer model to increased land surface roughness length
C C Heasman

DCTN 50 Feb 1987 The influence of atmospheric waves on the general circulation of the middle atmosphere
D G Andrews

DCTN 51 Feb 1987 Transport mechanisms in the middle atmosphere: an introductory survey
D G Andrews

DCTN 52 Mar 1987 The Met O 20 stratosphere-mesosphere model
M Fisher

DCTN 53 Apr 1987 Simulations of linear and nonlinear disturbances in the stratosphere
A O'Neill and V D Pope

DCTN 54 Apr 1987 Aspects of dynamics of the middle atmosphere inferred using data from a satellite and from a numerical model
T D A Fairlie and A O'Neill

DCTN 55 Apr 1987 The seasonal evolution of the stratosphere in the northern hemisphere
A O'Neill and V D Pope

DCTN 56 Apr 1987 The adjustment of numerical weather prediction models to local perturbations
B R Barwell and R A Bromley

DCTN 57 Jun 1987 Climate simulations for 9000 years before present: Seasonal variations and the effect of the Laurentide ice sheet
J F B Mitchell, N S Grahame and K J Needham

DCTN 58 Aug 1987 Climatic effects of nuclear war: the role of atmospheric stability and ground heat fluxes.
J F B Mitchell and A Slingo

DCTN 59 Oct 1987 The stratospheric major warming of winter 1984/85: observations and dynamical inferences.
T D A Fairlie and A O'Neill

DCTN 60 Oct 1987 Some comparisons between the middle atmosphere dynamics of the southern and northern hemispheres
D G Andrews

DYNAMICAL CLIMATOLOGY TECHNICAL NOTES

DCTN 61 Jan 1988 — Early winter in the northern stratosphere.
M N Juckes and A O'Neill

DCTN 62 Feb 1988 — Single column model tests of the Rowntree convection scheme using GATE data.
D Gregory

DCTN 63 Mar 1988 — The antarctic winter; simulations with climatological and reduced sea-ice extents.
J F B Mitchell and C A Senior

DCTN 64 Mar 1988 — An investigation of the Gates asynchronous coupling strategy using a simple energy-balance model.
D L Roberts

DCTN 65 Apr 1988 — The effect of improved physical parametrizations on simulations of cloudiness and the earth's radiation budget.
A Slingo, R C Wilderspin and R N B Smith

DCTN 66 May 1988 — Comparison of data and derived quantities for the middle atmosphere of the southern hemisphere.
W L Grose and A O'Neill

DCTN 67 Aug 1988 — Progress and future developments in modelling the climate system with general circulation models.
P R Rowntree

DCTN 68 Aug 1988 — A scheme for predicting layer clouds and their water content in a general circulation model.
R N B Smith

DCTN 69 Nov 1988 — Modelling climate change: an assessment of sea-ice and surface albedo feedbacks.
W J Ingram, C A Wilson and J F B Mitchell

DCTN 70 Dec 1988 — The "greenhouse" effect and climate change
J F B Mitchell

DCTN 71 Dec 1988 — On the dependence of climate sensitivity on convective parametrization.
W M Cunnington and J F B Mitchell

DCTN 72 Dec 1988 — Land surface parametrizations - basic concepts and review of schemes.
P R Rowntree

DCTN 73 Jan 1989 — Climate sensitivity: model dependence of results.
J F B Mitchell

DCTN 74 Jan 1989 — Parametrization of the upper ocean mixed layer in a tropical ocean GCM.
S Ineson and C Gordon

DCTN 75 Mar 1989 — A simple tropical coupled ocean-atmosphere model.
G R Budin and M K Davey

DYNAMICAL CLIMATOLOGY TECHNICAL NOTES

DCTN 76 Jun 1989 — The needs of general circulation models for runoff data.
P R Rowntree

DCTN 77 Jul 1989 — General circulation modelling of the atmosphere.
J F B Mitchell

DCTN 78 Jul 1989 — A model simulation of the seasonal cycle in the tropical Pacific Ocean using climatological and modelled surface forcing.
C Gordon and R A Corry